UNITED STATES DEPARTMENT OF THE INTERIOR
GEOLOGICAL SURVEY

Geology of the Veins and Vein Sediments, of the Golden Wonder Mine, Lake City, Colorado: an Epithermal Hot Springs Gold-Alunite Deposit

by

J. Kalliokoski[1]

and

Patty Rehn[2]

Open-File Report 87-344

This report is preliminary and has not been reviewed for conformity with U.S. Geological Survey editorial standards and stratigraphic nomenclature.

[1]Michigan Technological University
[2]1040 Serpentine Way, Sandy, UT

CONTENTS

ILLUSTRATIONS

TABLE

GEOLOGY OF THE VEINS AND VEIN SEDIMENTS OF THE GOLDEN WONDER MINE, LAKE CITY, COLORADO: AN EPITHERMAL HOT SPRINGS GOLD-ALUNITE DEPOSIT

By J. Kalliokoski and Patty Rehn

ABSTRACT

The Golden Wonder Mine is a small hot-spring-type epithermal alunitic gold-base metal deposit within flow-foliated rhyolite estimated between 27.1 and 28.5 M.Y., of the Oligocene volcanics of the Uncompahgre caldera. Mineralization probably took place during a period of extensive acid-sulfate alteration of the rhyolite, and is considerably older than an early stage sericite (20.8 m.y.) from the Ute-Ulay mine of the prevalent quartz-base metal mineralization that occurs in intracaldera fill of the Oligocene Uncompahgre caldera sequence.

In the upper mine levels, the rhyolite has undergone near-surface type acid-sulfate alteration (quartz ± kaolinite ± alunite) accompanied by pervasive silification that preserves primary volcanic textures. In the proximity of mineralization at the bottom level of the mine, the rhyolite has undergone advanced argillic alteration (quartz ± kaolinite ± illite), locally with massive alunite adjacent to the quartz vein.

Zoning is observed over a vertical interval of 120 meters: 1) veins of quartz + pyrite + marcasite at depth; 2) copper sulfosalts + base metal sulfides + pyrite; 3) base metal sulfides + pyrite + gold ± alunite ± kaolinite; and 4) base metal sulfides + tellurium and tellurides + alunite ± kaolinite at shallower depths. This vertical mineral zoning is superposed on three vertically stacked geologically distinct zones that are interpreted to have resulted from: (a) the local destruction of deeper parts of the rhyolite and of lower mineralized zones by wallrock alteration and sporadic explosive boiling; the upward hydrothermal transport of this debris as a slurry or by elutriation; (b) the deposition at shallower depths of unbedded breccias, bedded breccias, and quartzose sandstones in cavities; and, (c) the deposition in fault-controlled cavities still closer to the surface, of bedded alunite ± kaolinite, from a slowly moving hydrothermal fluid.

Quartzose sandstones fill fault-generated cavities. The quartz clasts were derived from quartz phenocrysts that were liberated from rhyolite during wallrock alteration and hydrothermal boiling. The sandstones also contain clasts of pyrite and chert, pellets of alunite, and irregular aggregates of anatase. The sediments are cemented by fine-grained quartz and alunite.

Microscopic native gold is common in quartzose sediments but rare in bedded alunite higher in the sequence. This distribution pattern suggests that gold may have been carried as a sulfide complex and was precipitated by the oxidation of the hydrothermal solution. The assemblage chalcopyrite + covellite + pyrite, and the abundance of fine-grained and skeletal pyrite in alunite bodies denotes that some of the sulfide deposition occurred under disequilibrium conditions when the solution was supersaturated in iron disulfide.

The Golden Wonder Mine exhibits many of the geological characteristics expected in a mineralized hot spring deposit: 1) a close spatial relationship with volcanic rocks with widespread acid-sulfate alteration of the host rhyolite; 2) localization of the sulfide mineralization generally below a near-surface zone of oxidation and silification; 3) association with hydrothermally brecciated rocks and veins, denoting episodic boiling; 4) occurrence of mineralized and unmineralized sediment as cavity fillings; 5) preponderance of bedded alunite at shallower levels; 6) the fine grain size of the opaque mineral suite denoting rapid precipitation; 7) the occurrence of a complex mineral suite within a relatively small vertical interval, consisting of native gold, base metal sulfides, copper sulfosalts, gold, silver, and nickel tellurides, and native tellurium.

INTRODUCTION

The Golden Wonder Mine is a small epithermal alunitic gold-base metal deposit, situated within the San Juan volcanic field of southwestern Colorado, about 3 km (2 miles) southeast of Lake City (fig. 1). The deposit is geologically unique among deposits in the area, and perhaps in the U.S. because gold mineralization is found in quartz sandstones that occur as open-space fillings in steeply dipping fault-generated cavities. The Golden Wonder deposit probably represents the mineralized upper part of a hot-springs system such as those described by White (1955, 1981) and Berger and Eimon (1982), a geological environment not generally exposed in underground workings, but here well-displayed (Billings and Kalliokoski, 1982; Kalliokoski and Billings, 1982; Billings, 1983). This paper will examine in particular the character and origin of these sediments and sediment-filled openings, and of the ore minerals within these sediments, as studied on the accessible third, fourth and sixth levels of the mine, and from the mine dumps. Most of the features photographed in dump samples correspond to similar but less photogenic features studied in the mine.

The deposit is zoned vertically, and a fairly consistent geological picture can be developed if one applies the hypothesis that the products of hydrothermal deposition in the shallower levels are slightly younger than those in the deeper ones.

In this study the first author was responsible for the details on the nature, extent, and controls on mineralization (Kalliokoski and Billings, 1982). The second author has provided information on the petrology and alteration patterns of the rhyolite (Billings and Kalliokoski, 1982; Billings, 1983).

Exploration and underground mining have been sporadic in the mine area since the discovery of the first veins in the 1880's (Irving and Bancroft, 1911). The Golden Wonder deposit is quite small, with a total pre-1978 production of "$40,000 to $50,000 principally in gold" (Slack, 1976), and probably has had an equally small subsequent production. The earlier production was from the zone of supergene oxidation that extends down to the third level (Delmar L. Brown, oral commun., 1981) and is not described in this paper. During 1980-1981 Lake City Mines, Inc., reopened the third and fourth levels and the connecting winze, stoped on the fourth level, drove the sixth level adit and the raise to the fourth level, and explored on the fifth and sixth levels (fig. 2) (Billings, 1983). These accessible workings comprise

the area of the present study. In 1982, LKA Minerals initiated a new exploration program, opening the first and second levels.

PREVIOUS STUDIES

Irving and Bancroft (1911) described the geology of the Golden Wonder Mine, and recognized that, in contrast to the open-space-filling veins that characterize other deposits in the Lake City district, the mineralization at this mine was different, suggestive of wallrock replacement.

Slack (1976) mapped the surface workings and outcrops as well as the then accessible third and fourth levels of the mine, agreed with the Irving and Bancroft interpretation of the character of the ores and noted the strong silification and argillization of the rhyolite host rock (quartz + muscovite + kaolinite + dickite, and both primary and secondary alunite). He noted that the ore pods on the fourth level were localized by narrow breccia dikes, that the ore occurs as thin (<1 cm) fracture fillings, as replacement pods and lenses, and as disseminations within, what he termed, massive jasperoid, and that this jasperoid (probably the silicified cavity-filling sediment of this paper) carries some of the best gold values in the mine. Slack also identified a large suite of ore minerals (table 1). He concluded on the basis of ore and host rock structures, textures, and mineralogy, that the deposit was genetically similar to the rich pipe- and chimney-ores of the Red Mountain district near Silverton, Colorado (Burbank and Luedke, 1968; Slack, 1976).

Hon and co-workers (1985) have been able to clarify some of the age and genetic relationships among the various types of mineral deposits in the Lake City district through a recently completed U-Pb isotope study of mineralized rocks at the nearby Golden Fleece Mine (fig. 1) and a review of existing isotopic, stratigraphic and structural data on mineralization.

GENERAL SETTING AND AGES OF MINERALIZATION

Veins of the Lake City area lie outside of the north and east margins of the Miocene Lake City caldera, but within the topographic boundary of the Oligocene Uncompahgre caldera (fig. 1) (Slack, 1976, 1980; Hon and others, 1983). The host rock at the Golden Wonder Mine is a rhyolite within the volcanics of Uncompahgre Peak, the upper part of the Uncompahgre caldera-fill sequence (Lipman and others, 1976). These rhyolites have undergone extensive regional acid-sulfate alteration. Their age is bracketed by the overlying volcanics of the Nelson Mountain tuff near Uncompahgre Peak (>27.1 ± 1 m.y.) and the underlying Fish Canyon Tuff (28.5 ± 1 m.y.) (Lipman and others, 1973; Lipman, 1976; also map relations).

In the nearby Golden Fleece Mine (fig. 1), the youngest assemblage, chalcedonic quartz and gold + silver tellurides + colloform pitchblende (Slack, 1976, 1980) has been dated by Hon and others (1985) at 27.5 ± 0.5 m.y., virtually identical to the age of the Volcanics of the Uncompahgre Peak host rocks (27.1 - 28.5 ± 1 m.y.). Further, they note that the vein is truncated by 23 m.y.-old lavas of the Lake City caldera. The only other dating of mineralization in the Lake City area has been of sericite at the Ute-Ulay Mine, located in Uncompahgre Caldera fill rocks 9 km (5 mi.) west of the Golden Wonder. This sericite gave a K-Ar age of 20.8 ± 0.4 m.y. and may

be related temporally to the Miocene Lake City caldera sequence (Slack, 1980; Hon and others, 1985).

Pb-isotope values for galenas from the Golden Wonder Mine (Doe and others, 1979) are distinct from those at the Golden Fleece Mine (Hon and others, 1985). Thus Hon and his co-workers suggest that, although of similar age, the Golden Wonder and Golden Fleece hydrothermal systems operated independently and without interaction. Furthermore, on the basis of Pb-isotopic ratios of galenas from veins containing the late barite-precious metal assemblage Hon and others (1985) suggested that these barite veins may belong to a still different hydrothermal system.

In summary, the Golden Wonder and the Golden Fleece veins appear to be associated with the Uncompahgre caldera (28 m.y.), whereas mineralization at the Ute-Ulay mine is probably related to the Lake City caldera (22.5 m.y.). Although probably nearly contemporaneous, the Golden Wonder and Golden Fleece deposits differ in mineralogy and structure and probably represent separate hydrothermal systems (Hon and others, 1985).

RHYOLITE HOST ROCK PETROLOGY

General

The rhyolite host rock at the Golden Wonder Mine is a portion of a dome-flow complex (Lipman, 1976). An early explosive phase of the complex, a rhyolitic tuff breccia has been recognized on the 6th level of the mine (fig. 3). The rhyolite varies locally in both grain size and texture, as could be expected in a series of flows. Flow foliation is locally pronounced and often steep adjacent to the mineralized structures. Elsewhere the foliation may vary to shallow dips or local convolutions (fig. 4).

Hydrothermally altered rhyolite

All of the rhyolite in the mine is altered, and two major types of altered rhyolite can be mapped that represent either two different types of alteration or kinds of rhyolites. One variety is silicified rhyolite that extends from the eastern end of the sixth level to the third level (figs. 4,5,6) and generally is more common where the host rhyolite is porphyritic. The silicified rhyolite contains quartz phenocrysts and has retained pseudomorphically such megascopic and microscopic textures as feldspar phenocrysts and flow banding (figs. 7,8). It is brownish gray to light gray, very hard under the hammer, structurally sound, and forms the walls for most of the sandstone pods. The mineral assemblage is quartz + kaolinite + alunite, with quartz constituting about 70 volume percent of the rock. There is no residual feldspar.

The other mappable type of altered rhyolite has fairly sharp contacts against the silicified variety, is generally light yellowish brown to white in color, soft, and structurally weak. Relic phenocrysts and flow banding are rare. On the third and fourth levels this altered rock contains a network of thin (1-10 mm) veinlets of fine-grained quartz, and some of the altered zones are bordered by 5 to 20 cm wide zones of disseminated pyrite (figs. 4, 6).

Near the mineralized zone, in the sub-level above the fourth level (fig. 6) dickite has been identified in the wall rocks, and illite occurs as a clay fill in an adjoining, unmineralized fissure. On the sixth level the wall rocks of the quartz-pyrite-marcasite vein are locally strongly alunitic.

The work of the second author indicates that the alteration at the Golden Wonder Mine is similar to that reported at several other hot springs-type systems including Borealis, NV (Strachan, D.G., et al., 1982), El Indio, Chile and Steamboat Springs, NV (Sigvaldason and White, 1962). Although the entire hot-springs system is not preserved, the portion from near the paleo-surface down to about 183 meters is present and has been exposed in the mine workings.

The most intense alteration occurs near the major vein structure (see figure 4; Billings, 1983) and decreases away from it and with depth. Three groups of alteration minerals have been identified, quartz-kaolinite-alunite (silification + acid-sulfate alteration), kaolinite-illite (advanced argillic), and sericite-kaolinite (argillic).

Quartz-alunite-kaolinite (silicification + acid-sulfate) alteration occurs near the vein structure. The silicified rhyolite is dark in color and non-porous. Primary flow foliation is, in some cases, obliterated. Kaolinite is ubiquitous, whereas, alunite occurs adjacent to small strucures and is most abundant approaching the major vein structure. The association of these minerals with unoxidized ore would indicate that they are hypogene.

On the 3rd and 4th mine levels the unsilicified rhyolite has been altered to kaolinite and illite with relict primary quartz. Alunite is present locally in minor amounts, often associated with a network of fine, punky quartz veinlets. This rhyolite is light colored and very soft.

On the deepest mine level, the 6th, the kaolinite-illite zone grades into a sericite-kaolinite zone. This alteration type differs from the kaolinite-illite zone in that relict sanadine is present and partly altered to sericite. Kaolinite is less abundant and occurs in the goundmass. Fine-grained, disseminated pyrite is locally abundant.

Some alteration contacts are indistinct and irregular, but many appear to be joints or shear surfaces, which in turn sometimes coincide with flow foliation. These contacts reflect the flow path for hydrothermal fluids. Consequently, it appears that the most important structures for localizing fluids were joints or shear surfaces which may have been formed during cooling of the rhyolite dome.

Silicification and acid-sulfate alteration occurred during the primary mineralization phase. The other two alteration types may have been later, during the waning stages of hot spring activity (Hemley, J.J., personal commun.). Alternatively, argillic alteration may also have occurred intermittently, due to seasonal fluctuations of the water table.

MINERALOGY

Methods of identification

A large suite of minerals has been identified from the Golden Wonder Mine (table 1). Some of the minerals are described in this section but others are

described subsequently in relationship to their specific geological occurrence. The primary and secondary minerals in the wallrocks have been identified by means of thin section petrography and X-ray diffraction. The opaque minerals are generally fine grained. (0.1 mm to 5 u). All have been studied in polished section, but it was possible to confirm the composition of only the larger ones by X-ray powder camera techniques. Some of the minerals in smaller grains have been analyzed semiquantitatively by electron microprobe as noted in the text.

Quartz

On the sixth and fourth levels fine-grained quartz occurs in symmetrical veins as an intergrowth with sulfides, or as a fracture filling. None of it is chalcedonic, or of the drusy, epithermal variety common elsewhere in the district. No fluid inclusions were found in any quartz from the mine.

A much finer-grained variety of quartz, here termed chert, occurs between the third and fourth levels as a greyish replacement of laminated sediments within the sandstone pods, and as a cement in coarse-grained quartz sandstone, siliceous pyrite breccia, and bedded breccia. In open spaces the material is microcolloform. Locally the breccias and sandstones have been so thoroughly cemented that the porosity has become plugged and the clastic texture obliterated.

Alunite

Alunite [$KAl_3(SO_4)_2(OH)_6$] is a major late-stage mineral in the deposit. It occurs as a wide-spread component in silicified rhyolite, as a pyritic mud in hydrothermally brecciated veins, in clastic pellets and rip-up chips in quartzose sandstones and breccias, as a cement in quartzose sandstone pods, as mineralized beds above quartzose sandstones, and as inclusions in sulfide grains.

X-ray diffraction study of the bedded alunite shows a range, for a, between 6.98 and 7.04AÅand for c, between 17.03 and 17.32AÅ classifying it as an aluminum-bearing variety of the alunite group (Botinelly, 1976). The alunite two-theta values for the 201 peak indicate that the alunite is potassic (Cunningham and Hall, 1976). Some material identified as alunite by X-ray diffraction contains detectable quantities of Sr, Pb, and P under microprobe scanning (suggestive of hinsdalite or svanbergite compositions), but may denote instead the occurrence of these elements in the alunite structure (Botinelly, 1976).

Hinsdalite

Slack (1976) identified hinsdalite [$(Pb, Sr)Al_3(PO_4)(SO_4)(OH)_6$] from this deposit by electron microprobe analysis. It has been identified in this study in three specimens by X-ray diffraction and comparing the resulting patterns with those of type hinsdalite (Michigan Technological University Museum No. DM3980).

Other minerals

The copper sulfosalts of this study have been identified by X-ray diffraction. Partial compositions of two were determined by electron microprobe analysis. Because of the incompleteness of these data, those

sulfosalts in the cubic series will be referred to as "tetrahedrite" and those in the tetragonal-(orthorhombic) famatinite-luzonite-(enargite) series as "enargite". Where more precise determinations permit, the specific mineral designation will be used without quotation marks.

Iron sulfide occurs as both pyrite and marcasite. These occur together principally on the sixth level. Most zinc sulfide is sphalerite, but in one alunitic specimen there are spherical bodies principally of sphalerite, with minor wurtzite.

Tellurium, sylvanite, and melonite, identified in polished section and by X-ray diffraction, occur as a fine-grained intergrowth in an alunite matrix, just above the fourth level, in the winze. Slack (1976) has reported tellurium-calaverite-melonite, but in quartz gangue, from a museum specimen attributed to the Lake City district only.

Supergene oxidation has affected the rocks sporadically along the main northeast drift on the third level, and the supergene mineral, tellurite (TeO_2) has been recognized in the winze, about 5 meters below that level. Other minerals that may be supergene in part are anglesite, covellite, hematite, and alunite.

STRUCTURES

Introduction

It can be demonstrated that some fractures and veins have localized the hydrothermal activity related to mineral deposition. These structures are described below.

Fractures and breccia dikes

The oldest pre-mineralization structures in rhyolite are fractures, parts of which are occupied by rhyolite breccia dikes composed of fragments of rhyolite (Slack, 1980). On the fourth and sixth levels there are many such breccia dikes (figs. 5, 6). They are as much as 1 m wide, but commonly parts of the fractures extend for many meters as hairline cracks. The fractures and breccia dikes are variable in strike and dip, but most show an easterly or northeasterly trend (Billings, 1983) similar to that of the barite-precious metal veins of nearby deposits. The breccia fragments are composed of silicified rhyolite, and the matrix is a dark fine-grained rock flour, variously altered to alunite and kaolinite, and locally with sparse to abundant disseminated pyrite, and trace amounts of marcasite, chalcopyrite, sphalerite, and anatase. Some, but not all, of the dikes have been silicified and pyritized after intrusion. At one location on the sixth level a one-cm clast of fine-grained pyrite in a breccia dike indicates the presence of an earlier stage of pyrite mineralization.

Vein fractures

There are in the mine workings about 20 branching veins, as much as 15 cm wide and a few tens of meters in length. On the east end of the sixth level the vein system follows and sub-parallels an earlier breccia dike (fig. 5).

Fault-controlled cavities

Small, fault- and fracture-controlled cavities, now filled by transported breccia fragments and sediments are exposed in the winze and on the fourth level (figs. 9 and 10). None were found on the fifth or sixth levels. These former cavities are tabular in shape, are as much as 2 meters wide, several meters in length along strike, and possibly 20 meters in height. The floor of one cavity is covered with several large (up to one meter) collapsed blocks of rhyolite wall rock that had fallen prior to filling of the cavity by sandstone. In the winze the cavities are localized along a host rock textural contact that strikes N. 60° E., and dips 60-70° northwest (fig. 9). It can be demonstrated for several of the sandstone-filled cavities that each was produced by a slight reverse movement along a steep fracture surface that ran parallel to the correspndingly steep textural contact within the rhyolite but locally cut across flow-layers in a series of step-like offsets, identical to a general structural setting for breccia pipes proposed by Mitcham (1974). By contrast, several of the chert-pyrite breccia bodies occupy spaces that are bounded by several steeply dipping, intersecting joints not related to textural contacts (fig. 6).

MINERALIZATION

General

Mineralization can be defined as encompassing the processes by which minerals are introduced into a rock, resulting in an economically or potentially valuable deposit (Gary and others, 1972). In the Golden Wonder deposit the process of mineralization is related to hydrothermal fluids from which opaque minerals were deposited by both chemical precipitation and clastic deposition (fig. 11). These depositing fluids are also interpreted to have destroyed locally, through boiling, earlier-formed mineralized veins, to have transported the resulting clastic material (including sulfide fragments) into cavities, and then, still later, to have precipitated ore minerals into these sediments. Some of the processes recurred more than once. Consequently, the character and patterns of mineralization in this mine differ markedly from those encountered in most hydrothermal deposits. To emphasize these differences the succeeding pages will describe, in paragenetic sequence, the general nature of the materials that were deposited from the hydrothermal fluids.

Two types of early mineralization can be recognized: veins consisting of fine-grained quartz-pyrite-marcasite along fractures, and at slightly shallower levels in the mine, coatings of thin crusts of "tetrahedrite" on walls of tabular, open cavities. Both types exhibit kaolinitic wallrock alteration and were affected locally by late intense alunitic wallrock alteration and hydrothermal brecciation. This second type of mineralization occurs on walls of cavities within which bedded sandstone and alunite were later deposited.

There are also two types of later mineralization, both in sediments; one consists of base metal sulfides with native gold, within quartzose sandstone pods, and the other in bedded alunite, of base metal sulfides, selenides, and tellurides with no native gold.

Veins

The deepest, and presumedly earliest, stage of mineralization is represented by veins of quartz-pyrite-marcasite as much as 15 centimeters in width and a few tens of meters in length, that occur on the fourth and sixth levels, generally along branching fractures. On the sixth level (fig. 5) the rhyolite wallrocks are altered to quartz + kaolinite with disseminated pyrite, and silicified along the vein margins. The veins are encrusted with as much as several centimeters of one or more colloform layers of pyrite, alternating with fine-grained polygonal quartz (fig. 12). There is minor "tetrahedrite" and sphalerite. In the widest part of the vein the youngest sulfide layers are either marcasite or a mixture of pyrite and marcasite.

Locally on the sixth level a period of later hydrothermal alteration has converted the wallrocks of these veins to massive alunite, resulting in a structural weakening of the walls (fig. 13). Thus, along strike the vein changes from a planar feature on the west, where the rocks have retained their structural integrity, to folded and dismembered material on the east, where the wallrocks are strongly alunitized and have become structurally weakened permitting deformation.

In the zone of most intense alteration, the vein terminates as a mass of secondary breccia that consists of a resistate assemblage of fragments of vein quartz, pyrite, and silicified rhyolite, all in an alunite matrix (fig. 13). Alunite, with abundant skeletal and rounded bodies of pyrite and marcasite (about 10u in diameter) is present in the central vug along the less deformed part of the vein (fig. 12). Within the vein and in the adjacent hydrothermal breccia are thin veinlets of still younger pyrite and marcasite, some metallic yellow and others a very fine-grained black powder. A similar multi-stage history for early pyrite is represented by its deposition in breccia dikes, and the occurrence of pyrite as clasts in other breccia dikes.

Coatings

On the fourth level and in the winze there is a distinctive stage of mineralization represented by a thin (1-3 mm), dark mineral coating on walls of cavities that were subsequently filled by sediment and further mineralized (3, fig. 11). On walls of cavities now filled predominantly by quartz sandstone (fig. 14) the crustified coating consists of "tetrahedrite" with included "enargite", chalcopyrite, native gold, and petzite. In the sublevel above the fourth level (fig. 6) where the sediment filling is alunitic, the encrustations consist of a succession of layers, from wall inward, of: "tetrahedrite"-chalcopyrite; sphalerite-chalcopyrite with inclusions of luzonite ($\underline{a}$ - 5.28A; $\underline{c}$ - 10.44A) (Luce and others, 1977); galena with inclusions of chalcopyrite, gold and alunite, locally some galena altered to anglesite and covellite; and sphalerite in contact with the alunitic sediment filling.

A stage of subsequent hydrothermal alteration and brecciation is documented by also one of the coating occurrences. In the sublevel above the fourth level (fig. 6) a thin crust of sulfosalts and sulfides outlines a pod of alunitic sediment a few centimeters wide and decimeters high. The pod occurs along a zone in which the wall rocks have been altered to quartz + kaolinite, with local dickite and small quantities of alunite, and have become

so soft that the originally continuous crust of ore minerals now occurs as broken segments in a clayey alunite matrix.

Chert-pyrite breccia

Several small, pipe-like and tabular bodies of chert breccia occur in the winze and on the fourth level (figs. 6, 9 and 10). Some of these are isolated bodies in silicified rhyolite while others adjoin, but pre-date bodies of quartzose sandstone (fig. 11). The breccias consist of angular to subangular fragments as much as two centimeters in diameter of predominantly light gray chert and highly silicified rhyolite, with lesser amounts of rounded to angular clasts of vein-type and replacement-type pyrite and pyrite-marcasite, and still less abundant grains of sphalerite, "tetrahedrite", and galena, all of which are cemented by cherty quartz (fig. 15). In some bodies the quantity of pyrite is quite small. Most of the pyrite within breccia masses has a demonstrable clastic texture and distribution. No hydrothermally deposited post-breccia ore-minerals have been recognized, and consequently all of the opaque minerals in these breccias are interpreted to be epiclastic.

Quartzose sediments and epiclastic sulfides

Bedded quartzose sediment bodies occur as cavity fillings of fault-generated voids (figs. 9,10,11). Three such sandstone bodies have been identified in the mine, and similar material occurs on the dumps below the second level adit. This distribution suggests a maximum vertical range of about 70 meters for such sandstone in cavities at this mine. Some of the sandstone bodies in the winze were deposited against an earlier chert-pyrite breccia mass, and some are overlain by bedded alunite (figs. 9, 11). These quartzose sandstones range in grain size from silt to coarse sand, and to conglomeratic sand, but will be referred to generally as "sandstone".

Much of the sediment is light to dark colored quartz sandstone, the color variation denoting differences in grain size, matrix composition, and in the amount of epigenetic sulfide present along bedding planes (fig. 14). The sediments occur in subhorizontal beds that locally are cross bedded (figs. 10,16), and have scours at the base of beds, lenticular beds and abrupt vertical variations in grain size between adjacent beds (figs. 10, 17). On the fourth level some beds are up to one meter in length. The sediment beds abut the wallrocks (figs. 10,14) and in places show a slight amount of shearing or dragging of beds along the walls (fig. 14), suggestive of differential compaction.

Most of the sand grains are composed of quartz, as large as 1.5 mm in diameter (figs. 17,18). Many are sub-rounded and show deep marginal embayments, similar to the quartz phenocrysts in the host-rock rhyolite (fig. 8), some are idiomorphic, and a few contain probable devitrified glass inclusions. Others exhibit a small amount of diagenetic overgrowth.

The sandstone bodies contain an epiclastic suite of transported minerals, including rounded grains of pyrite; clots and pellets of alunite; clots of kaolinite; and prismatic grains and irregular aggregates of anatase, or anatase-pyrite, some the pseudomorphically replaced remains of original ilmenite-magnetite. The matrix cement both in sandstones and quartz siltstones is fine-grained quartz with alunite and minor kaolinite.

In the sandstone pods there are a few kaolinite-alunite (fig. 19) and alunite beds. The kaolinite and alunite in the beds, and perhaps even in the matrix, is interpreted to have precipitated out of the overlying water column, flocculated, and then settled to the bottom, rather than being an authigenic cement derived by crystallization from a pore fluid.

Many quartz grains resemble quartz phenocrysts from the host rhyolite in morphology, size, and content of glass inclusions. These clasts could not have been derived from phenocrysts within the silicified rhyolites because these rhyolites are too uniformly cemented with silica to permit the selective liberation of quartz phenocrysts as clasts. Thus the grains are inferred to have been derived from non-silicified wall-rocks along a deeper part of the hydrothermal system.

Interlayered with the sandstone beds, or laterally adjacent to them, are coarse layers of crudely bedded breccia consisting of equidimensional to platy chert clasts (figs. 17, 20). The clasts are as much as several centimeters in size, and are of various shades of light to dark gray, depending on the degree of later silification. A few can be identified as rip-up clasts of earlier, alunite-cemented quartz siltstone.

The bedded breccias are silica-cemented, and pore spaces are partly to completely filled, obliterating the clastic textures (fig. 17). However, for the most part the resulting fabric still contains voids or open spaces up to 2 mm in diameter, some of which were later filled with kaolinite. Locally, the original porosity is preserved in subhorizontal zones a few tens of centimeters long in the breccia layers (figs. 16, 20). On the fourth level there are also irregular open cavities as much as 30 cm in their maximum dimension. Commonly the clasts of chert in the channels are coated by one or more thin (<1 mm) layers of cherty quartz, with or without intervening films of "tetrahedrite." Later some of these channelways were filled with 1-5 mm sized clastic debris, some of which escaped subsequent cementation, and on the fourth level large cavities were partly filled with clay.

Epigenetic ore minerals in quartzose sediments

An economically important epigenetic suite occurs in the sandstones as a fine-grained concentration and dark pigmentation along the bedding planes (fig. 14), and in places along cross bed foresets (fig. 21). The largest grains are pyrite (0.1 mm) and some beds contain sufficient native gold to produce assays up to 20 oz/ton (Delmar L. Brown, oral commun., 1981).

Some pyrite occurs as small replacement bodies or grains, a few centimeters in size, with minor inclusions of "tetrahedrite." More commonly pyrite occurs as 10 to 100u cubes, generally concentrated along particular cross bed foresets (fig. 21). None of the pyrite is of the spherical, radial, or skeletal types that are common in the alunite bodies in this deposit, and there is no marcasite.

The other opaque minerals occur as single crystals and as intergrowths, but their fine grain size (5-50u) has prevented the identification of all the phases using only optical and X-ray diffraction techniques. However, the more abundant minerals are pyrite; chalcopyrite with discontinuous zones of covellite; chalcopyrite intergrown with "tetrahedrite"; sphalerite;

"tetrahedrite" ± "enargite"; galena; native gold; and possibly petzite. Some chalcopyrite contains covellite and locally, a mixture of covellite and minor earthy hematite. The assemblage of ore minerals varies in relative and total abundance of phases from one bed or crossbed set to another, and locally even from one crossbed foreset to the next.

Native gold is rare in some conspicuously crossbedded, alunite-poor sediments. Conversely, along some layers in less well bedded sandstone, some of which contain small, white spots of kaolinite and minor alunite, specks of gold are visible in almost every field of view under 125X magnification. None of the gold is visible megascopically.

Gold has three typical habits in quartzose sandstone, all of which may appear within a single polished section: 1) as rare inclusions in copper sulfosalt, 2) isolated, somewhat oval 1-100u grains; and 3) as inclusions in, and free grains near, chalcopyrite, particularly where the chalcopyrite has been altered to an aggregate of covellite and fine-grained hematite. This third type may denote late oxidation.

Sedimentary alunite

Bodies of bedded brown alunite occur in the winze below the third level (figs. 9, 10), and on the fourth level (fig. 6). These deposits occur in the upper parts of the same cavities that contain quartzose sediments in their lower parts. The contact between alunite and the underlying bedded sandstone is horizontal and fairly abrupt. However, sandstone pods contain thin beds of alunite in their upper parts, and all sandstones contain alunite as a matrix component. Also, in some dump samples, bedded alunite contains thin layers of sand-sized breccia.

Bedding in alunite is manifested by slight color variations between beds (fig. 22). In places the beds are offset on faults, perhaps produced during compaction. Other beds are contorted caused by soft-sediment deformation, are brecciated suggesting a post-consolidation deformation, or show alunite of one color truncating alunite of another color, perhaps denoting syn-sedimentary alteration or soft-sediment deformation (fig. 23). The smallest bodies of bedded alunite along a single fissure at the southwest end of the fourth level are disc-shaped, and each pod is about 1 meter in the greatest dimension (a, fig. 6).

In the winze, cauliflower-patterned clusters of light cream colored alunite, as much as 1 cm in diameter, occur in a matrix of darker alunite, both cut by hairline alunite veinlets (fig. 24). The light colored alunite spheres forming the clusters are flattened horizontally, suggesting soft-sediment deformation, and may represent diagnetically replaced kaolinite.

Mineralization in bedded alunite

There are two kinds of mineralization in bedded alunite: 1) small volumes of breccia with elongate epigenetic fragments of colloform sulphide crusts in an alunite matrix, that probably accumulated from brecciated cavity linings, and 2) conformable, convex upward layers of colloform sulfides interbedded in alunite sequences, denoting that periods of basemetal sulfide

precipitation alternated with periods of predominant alunite sedimentation in the same open, water-filled cavity (fig. 22).

These crustiform sulfide layers and elongate fragments consist of chalcopyrite, sphalerite, galena, and pyrite, commonly with small included plates of alunite (fig. 25). Many of the microcolloform chalcopyrite grains contain discontinuous zones of covellite, and also inclusions of tellurobismuthite (confirmed also by powder camera), possible wehrlite, and other still incompletely analysed minerals in the Bi-Te-Se-S system. Electron microprobe analysis has disclosed inclusions within sphalerite of probable luzonite. Galena is a common minor constituent in the alunite matrix, but in some specimens most of the galena has undergone alteration to anglesite (fig. 26). Just above the fourth level native tellurium occurs as fine-grained intergrowths with sylvanite and melonite in an alunite matrix (fig. 27). Slack (1976) has reported tellurium-calaverite-melonite from the Lake City district but in a quartz gangue.

Spherical and skeletal forms of strongly anisotropic and isotropic pyrite are common in bedded alunite (figs. 26, 28) but no marcasite could be identified by X-ray diffraction. However, veinlets of late colloform pyrite-marcasite do occur in the winze around some brecciated alunite bodies.

Elsewhere in the bedded alunite are small bodies a few centimeters in size, consisting of an aggregate of sphalerite-wurtzite spheres that show a zonation caused by a variable content of included platelets of probable alunite (fig. 29). There are also clusters of chalcopyrite-alunite in which the chalcopyrite shows convex outer boundaries against the alunite, suggesting control on morphology by the higher surface energy of chalcopyrite in relation to that of the alunite matrix (fig. 30).

INTERPRETATIONS

The textures and compositions of the materials affected by the hydrothermal fluids permit interpretations regarding the hydrothermal system.

Evidence for two types of fluids

The most conspicuous and pervasive wallrock alteration is the silification produced by the conversion of the felsic volcanic rocks to quartz+kaolinite+alunite. This assemblage resembles in mineralogy and near-surface occurrence the acid sulfate alteration that is common in shallow hydrothermal systems (fig. 31). In these the permeability has been reduced to the extent that net groundwater recharge no longer keeps up with net hydrothermal discharge (White and others, 1971). Consequently, the system changes from hot water to steam, the steam is condensed by perched groundwater (Lloyd, 1959), and the groundwater acquires a low pH by the near-surface oxidation of hydrothermally introduced H_2S, as at Steamboat Springs (Schoen and others, 1974). In hot spring environments the entire system is warm, probably enhancing the devitrification of glass. The low-pH, oxidizing, supergene water migrates downward, breaks down feldspars, and depending on its acquired concentrations of silica, potassium, and sulfate, precipitates quartz, kaolinite, and alunite in the alteration blanket (Knight, 1977). This is the proposed origin for the quartz+kaolinite+alunite alteration at the mine (figs. 11, 31). This process was not related in any direct way to the introduction of ore minerals into the deposit.

In the soft rhyolite, the alteration mineral assemblages are quartz+sericite+kaolinite with relict sanidine, and quartz+kaolinite+illite. The first assemblage is suggestive of such argillic alteration as described from Butte, Montana, whereas the latter resembles assemblages characteristic of zones of advanced argillic alteration, closer to the vein, both related to an ascending, reducing hydrothermal fluid. (Meyer and Hemley, 1967). Dickite and illite, identified from near the mineralized zone also are diagnostic of the advanced argillic type of wall rock alteration (Meyer and Hemley, 1967, p. 170). At the Kasuga Mine in Japan an epithermal gold deposit, the inner, mineralized zone is alunitic, and outward the wall rocks show a zonal sequence of dickite-kaolinite, and kaolinite (Boyle, 1979, p. 268, 270). The zonal pattern at the Golden Wonder Mine suggests that the wall rock alteration and mineralization may have been related to the same ascending fluid.

The second author feels that a perched gound water table is not necessary for the evolution of fluids at the Golden Wonder Mine. The concept of two discrete fluids seems too simplistic for a system where sulfate and sulfide phases seemingly coexist. Previous work which indicates alunite as a supergene phase may not apply to all alunite in all hot springs, particularly at the Golden Wonder where alunite exists as a vein-filling mineral. Perhaps it is more enlightening to consider the evolution of hot springs as continuum in both time and space. Modern hot springs, such as Yellowstone, illustrate how complex the situation may be. Active springs are adjacent to steaming ground which may in turn abut an active geyser. A few months later the springs may all have dried up or the steaming ground could have new mud volcanoes. All the while, the fluids are continuously evolving--boiling, condensing, and changing in concentration.

Evidence for explosive hydrothermal activity

The earliest fracture fillings are breccia dikes that occur on the sixth and fourth levels (figs. 5, 6, 31). These kinds of breccia dikes fall into the class interpreted by Sillitoe (1985) to be the product of phreatic fracturing of rock and the filling of these fractures by rock debris. Some of the later fractures filled by early quartz-pyrite-marcasite follow the trend of these breccia dikes, suggesting that these fractures also may have been produced by phreatic fracturing (fig. 31). The relationships among breccia dikes, faults, and hydrothermal and clastic pyrite in the breccia dikes suggest that at least two periods of such fracturing were separated by a period of pyrite deposition.

The brecciation and destruction of earlier mineralization has occurred also along parts of the quartz-pyrite-marcasite vein on the sixth level (fig. 13) and in the "tetrahedrite"-lined cavity above the fourth level (fig. 6), both succeeded by alunite deposition. This brecciation, intense wall rock alteration, and alunite deposition are interpreted to represent near-surface steam explosion and in-flow of supergene, oxygenated water into a hot, hydrothermal conduit (fig. 11). These two occurrences show a 70 meter difference in elevation, suggesting this distance as the minimum vertical interval in which this process took place.

No fluid inclusions were found in quartz or sphalerite to provide an estimate on the temperature of the hydrothermal fluids. However, should the present depth of mineralization on the sixth level, about 340 meters below the

present top of the rhyolite of the volcanics of the Uncompahgre Peak (Lipman and others, 1976), approximate the original depth, one can estimate that corresponding boiling was initiated in this hydrothermal system near 235°C.

On the sixth level the process that involved vein brecciation left behind in the vein the larger, siliceous, iron sulfide-rich fragments as a heavy-residue concentrate, and possibly removed the smaller breccia fragments by elutriation.

Evidence for fluid movement

The hydrothermally brecciated vein on the sixth level, consisting of a resistate assemblage of vein and silicified wallrocks material resembles the isolated bodies of chert-pyrite breccia higher in the Golden Wonder Mine (fig. 13). Likewise, the elongate breccia fragments of basemetal sulfide encrustations above the fourth level resemble those seen as conformable layers in alunite bodies higher in the winze and in dump specimens. This evidence suggests that the brecciated material may have been derived and transported from depth in hydrothermal conduits, either by high velocity, low density steam, or as a slurry of lower velocity, higher density fluid, as suggested elsewhere for ore transport by Anderson (1974).

The sandstone bodies consist principally of clastic quartz, up to 1.5 mm in diameter. As noted above, the quartz sand grains are probably relict rhyolite phenocrysts, similar to those described from the Montana Tunnels diatreme-hosted gold deposit in Montana by Sillitoe and others (1985). It is proposed that, at the Golden Wonder, during advanced argillic alteration of unsilicified rhyolite, perhaps accompanied by periodic boiling and steam explosion, phenocrysts became liberated from a clay-rich matrix and available for transportation and to sorting by elutriation. The other clastic grains may have been derived in a similar manner from the deeper rhyolite strata.

Cross bedded sandstone denotes deposition under varying conditions of current velocity and sediment supply. The fact that the cross beds show variations in dip direction suggests that both the point of discharge of sediments into the cavity and the direction of the depositing current flow were variable. Clearly, there was a certain amount of lateral transport of sediment within the cavity, but its extent is indeterminate.

The rare interlayers of bedded breccia in sandstones suggest that both have similar modes of origin. However, the breccia beds were deposited from a much higher velocity flow, and the rip-ups and the variety of clasts in these breccias denote that the clasts were eroded and transported from several sources.

The delicately bedded alunite represents the filling of the remaining open space above quartzose sandstone by the settling of chemically precipitated alunite from water that was either still or flowed much more slowly than the water that transported the clastic quartz.

CHEMICAL CONDITIONS DURING ALTERATION AND MINERALIZATION

The Golden Wonder mineral deposit occurs in rhyolite that has undergone argillic hydrothermal alteration at depth and acid-sulfate alteration closer to the surface. The general position of the argillic-altered lavas (quartz+sericite+kaolinite; quartz+kaolinite±illite) on a log fS_2/log fO_2 plot (fig. 32) can be represented by point a. The chemical conditions initiating the predominant alunite deposition can be represented by point b. The large difference in both fO_2 and pH between these two systems points to the possible presence of two fluids, a deeper one that is more reducing and sulfidizing, and a shallower one that is more oxidizing. The change in both fO_2 and pH from a to b can be explained by the infiltration of the deeper system by the more oxidizing near-surface water.

The mineral deposit shows vertical zoning in both its mineralogical and physical characteristics, pointing to corresponding vertical gradients in the chemical and physical parameters. Features suggestive of chemical non-equilibrium during mineralization are the spherical and skeletal forms of pyrite in alunite pods, and the very fine grain size of many minerals including the opaques, cherty quartz, and alunite. These have been suggested as criteria for precipitation under conditions of supersaturation (Barton and others, 1977). The intergrowth of sphalerite and wurtzite also represent crystallization under disequilibrium conditions. Such chemical disequilibrium conditions may arise from rapid cooling, boiling of the hydrothermal solution, or mixing of hypogene and supergene solutions (Browne, 1984).

The association of chalcopyrite with covellite in alunite pods (fig. 25) can be explained as a further consequence of pyrite disequilibrium during mineralization. Vaughan and Craig (1979, p. 258-259, 303) noted that the occurrence of chalcopyrite with covellite signifies that pyrite concentration in solution exceeded its saturation limit by a factor of ten. Thus, the covelite with chalcopyrite in the Golden Wonder probably can be designated as "hydrothermal," but it is not at all clear whether, or to what extent, the mineralizing solution was a mixture of ascending and descending fluids.

The predominant sulfide in the deepest-exposed veins is pyrite, with kaolinite in the wallrocks (fig. 10). The general position for this assemblage on a log fS_2/log fO_2 plot (fig. 32) lies near a. The change to the assemblage pyrite-marcasite may denote a lowering of pH, which would tend to favor the growth of marcasite (Reynolds and Goldhaber, 1983). Such a lowering of pH could be caused by an influx of more oxidizing near-surface acid-sulfate water.

The crusts of copper sulfosalts on cavity linings from the fourth level represent a slightly shallower type of mineralization. Knight (1977) pointed out that in a hydrothermal system in which alunite is deposited near the surface and sulfide minerals are deposited at depth, the decrease in temperature upward will favor the deposition of copper sulfides over iron sulfides, and enargite (luzonite) and tennantite over copper sulfide minerals.

After the brecciation of these veins, an alunite mud, without kaolinite, but with abundant microscopic skeletal crystals of pyrite, precipitated from these solutions and settled around the fragments. The chemical conditions initiating this alunitic alteration and precipitation may be represented by point b in figure 32. The shift from a to b suggests a possible infiltration

of low pH near-surface water. In log aO_2/pH space this change is depicted by the line a-b (fig. 33.b).

The occurrence of a gold-bearing base metal suite in quartzose sandstones and of a gold-poor assemblage in the alunite bodies also can be explained by the chemical interactions between a more reducing, mineralizing, water body situated below a more oxidizing one. In the quartz sandstones the critical mineral assemblage is anatase-pyrite, derived from the alteration of epiclastic ilmenite-magnetite intergrowths. In these the magnetite phase has altered to pyrite, and hematite is absent. Thus, magnetite is unstable with respect to pyrite (figs. 32, 33). In fS_2 and fO_2 space (fig. 32) the system can be designated by point a.

Gold can be transported as sulfide, telluride, chloride, or thioarsenide complexes (Barnes, 1979; Casadevall and Ohmoto, 1977; Henley, 1973; Seward, 1973; Romberger, 1982, 1986; and Henley and Ellis, 1983). However, these systems are still so poorly understood that they provide little more than general guidance to speculation. The stability field of predominant sulfide complexes of gold lies almost entirely within the pyrite stability field (fig. 33) (Casadevall and Ohmoto, 1977; Barnes, 1982), and near the alunite-pyrite boundary gold solubilities decrease precipitously in the direction of increasing oxygen fugacity or lower pH (fig. 33a, b). By contrast, gold chloride complexes predominate in the alunite field, but their solubilities increase toward values of lower pH and higher fO_2 (fig. 33a, b). These complexes are also several orders of magnitude less efficient in transporting gold than are the sulfide complexes. Thus the general geological setting and the prevalence of pyrite favor the view that between the third and sixth levels of the Golden Wonder Mine the gold may have been transported as sulfide complexes, and became precipitated by oxidation of the solution (figs. 32, 33; path a-b). The tellurium- and arsenic-bearing mineral phases in the deposit suggest that the geochemistry of the gold-transporting system probably was considerably more complex than what has been depicted above.

Oxidation of the solution may have taken place either by mixing with low pH near-surface waters, a mechanism favored by many (for example, Henley and Ellis, 1983), or by boiling (Drummond, 1981). Mixing (figs. 32, 33; path a-b) would explain the minor quantities of alunite and/or kaolinite in the gold-bearing material in the quartzose sandstone, and the absence of gold in bedded alunite.

A major remaining problem concerns the origin of several sulfides and sulfates such as covellite, alunite, and anglesite, the deposition of which seems to span the transition from reducing and sulfidizing solutions to more oxidizing ones. Our present level of understanding corresponds to the comment of Hemley and others (1969) that in some epithermal deposits the geological distinction between supergene and hypogene alunite becomes ambiguous. Neither do we know whether the sulfate was derived by oxidation of near-surface pyrite or from hypogene H_2S, or both (Slack, 1976).

COMPARISON WITH HYDROTHERMAL AND KARST SYSTEMS

Alunitic gold deposits are a characteristic group among the epithermal class (Lindgren, 1933), their relationship to hot springs has been well documented (White, 1955, 1981) and their major features have been modelled

(Berger and Eimon, 1982; Kesler and others, 1981; fig. 31). The Golden Wonder Mine also falls into the hot springs category on the basis of geological setting in young volcanic rocks, wallrock alteration (advanced argillic, and supergene-acid-sulfate with near-surface silicification), and the presence of phreatic breccia dikes and hydrothermal breccias. It differs from epithermal vein deposits in the occurrence of sediment-filled veins and in the mineralization of these sediments. These features are interpreted to denote the shallower setting of a hot springs system where episodic boiling and phreatic explosions produced and transported the sediment. The closest analogy may be with the probably even shallower Borealis epithermal gold deposit in Mineral County, Nevada, where open pit workings have disclosed mineralized spring vent sediments, sulfide-cemented quartz breccias, and a hot springs discharge apron (Strachan, and others, 1982).

In this shallow hot-springs environment there can be broad variations in the types and rates of interactions between the more reduced hypogene, thermal waters and the lower pH, more oxidizing supergene waters, which in turn are related to such characteristics as wall-rock permeability, rates of recharge and discharge, thermal gradient, or the relative chemistries of the two water bodies. However, certain features are prominent: the fine grain size of the minerals and certain mineral relationships suggest that mineral deposition was rapid, equilibrium possibly was not always achieved, and some minerals cannot be designated readily as either hypogene or supergene.

The Golden Wonder mineralized hot springs deposit is marginally economic, but encourages a search in the surrounding area for similar but larger and richer mineralized paleo-hot spring systems. Exploration criteria that might help identify such a mineralized system are a near surface geochemical halo (White, 1981), and an effective fluid mixing environment such as that associated with a hydrothermal explosion vent, or with near-surface open fissures in a favorable near-surface paleogeohydrologic system (Henley and Ellis, 1983) particularly in proper geological relationship to the near-surface silicification blanket.

Subterranean accumulation of sediments is not unique to hot-spring systems, because such sediments can accumulate in a variety of environments. For example, the superposition in karst systems, of clay-sized sediment above coarser fluvial sediments (Drew and Cohen, 1980) resembles the situation at the Golden Wonder Mine. However, at the Golden Wonder Mine, most of the fine-grained alunite and kaolinite are interpreted to have originated by precipitation and possible elutriation within the hydrothermal system. Only illitic clay in the sublevel above the fourth level may be of the transported type that Bull (1978) has defined as "allochthonous". By contrast, in cave systems the clays that overlie the current-transported sands and gravels are thought to represent either a transported sediment derived by erosion and/or residual concentration from a variety of source rocks (Bull, 1981; White and White, 1968) or to represent hydrothermal replacement of wall rock (Monroe, 1973). Other, occurrences associated with subterranean sediments include karst and subterranean systems that contain small bodies of epiclastic sulfides such as those at Jefferson City, Tennessee (Kendall, 1960), later epigenetic sulfides that were deposited in and around sand bodies produced by hydrothermal leaching and redeposition along subhorizontal manto channels such as at Gilman, Colorado (Lovering, 1958); cavity-filling sediments that post-date fluorite veins such as at Maine, France (Joseph and Tournay, 1974), and

steeply inclined paleosinkhole fillings with later exceedingly rich, sulfide mineralization around the periphery of the pipe such as at Tsumeb, Southwest Africa (Button and Tyler, 1981; Sohnge, 1963).

ACKNOWLEDGEMENTS

We wish to extend our thanks to M.W. MacGuire, then the President of Lake City Mines, Inc., and to J.V. Vickers, owner of the property for granting access to the Golden Wonder Mine; to Delmar L. Brown for background information on the mine; to John Tinsley for introduction to the voluminous literature on cave sediments; to Allan Kirk, Rick Sanford, Steve Ludington, Skip Cunningham, and Ken Hon for careful critiques that lead to improvements to the manuscript; to our colleagues, R.L. Grauch, B.F. Leonard, Ralph Christian, Charles Lake, Rick Sanford, Skip Cunningham, and Tom Nash for help and guidance; and to Felix Mutschler for his suggestion that the textures could be indicative of a hot springs environment.

The field study and some of the laboratory work by one of us (J.K.), and all of the work by the other (P.R.) was supported by the U.S. Geological Survey. Support for additional laboratory work (J.K.) at Michigan Technological University came from departmental funds, with unstinting help provided by R. McCarthy, Rod Johnson, and Julene Erickson. To all, our thanks.

REFERENCES CITED

Anderson, Roy A., 1974, Slurry injection of vein materials in the Coeur D'Alene district: Economic Geology, v. 69, p. 414-415.

Barnes, H.L., 1979, Solubilities of ore minerals, in Barnes, H.L., ed., Geochemistry of hydrothermal ore deposits: New York, Wiley-Interscience, p. 404-460.

_____1982, Solubility of gold at 100°C and 250°C: in Alvin Lervis, assoc. editor, Gold geochemistry: Engineering and Mining Journal, v. 183, no. 12, p. 60.

Barton, Paul B., Jr., Bethke, Philip M., and Roedder, Edward, 1977, Environment of ore deposition in the Creede Mining District, San Juan Mountains, Colorado: Part III. Progress toward interpretation of the chemistry of the ore-forming fluids for the OH vein: Econ. Geol., v. 72, p. 1-24.

Berger, Byron R., and Eimon, Paul I., 1982, Comparative models of epithermal silver-gold deposits: SME-AIME Ann. Meeting, Dallas, Feb. 14-18, 1982, Preprint 82-13, 25 p.

Billings, Patty, 1983, Underground geologic maps of the Golden Wonder Mine, Lake City, Hinsdale County, Colorado: U.S. Geological Survey Open-File Report 83-0907, 1 sheet.

Billings, Patty, and Kalliokoski, J., 1982, Alteration and geological setting of the Golden Wonder Mine, western San Juan Mountains, Colorado: Geol. Soc. America Abstracts, v. 14, no. 7, p. 443-444.

Botinelly, Theodore, 1976, A review of minerals of the alunite-jarosite, beudantite, and plumbogummite groups: U.S. Geol. Survey Jour. Research, v. 4, p. 213-216.

Boyle, R.W., 1979, The geochemistry of gold and its deposits: Geol. Survey Canada Bull., 280, 584 p.

Browne, Patrick, 1984, Occurrence of ore minerals in some terrestrial geothermal systems: SME-AIME Ann. Meeting, Los Angeles, Feb. 26-Mar. 1, 1984, Preprint 84-73, 7 p.

Bull, Peter E., 1978, A study of stream gravels from a cave: Agen Allwedd, South Wales: Zeitschrift fur Geomorphologie, Berlin-Stattgart, v. 22, no. 3, p. 275-296.

_____1981, Some fine-grained sedimentation phenomena in caves: Earth Surface Processes and Landforms, John Wiley and Sons, Ltd., v. 6, p. 11-22.

Burbank, W.S., and Luedke, R.G., 1968, Geology and ore deposits of the western San Juan Mountains, Colorado, in Ridge, J.D., Ore deposits of the United States, 1933-1967 (Graton-Sales Vol.): New York, Am. Inst. Mining Metall. Petroleum Engineers, v. I, p. 714-733.

Button, Andrew, and Tyler, Noel, 1981, The character and economic significance of Precambrian paleoweathering and erosion surfaces in South Africa, in Econ. Geol. Seventy-Fifth Anniversary Vol., p. 687-709.

Casadevall, Tom, and Ohmoto, Hiroshi, 1977, Sunnyside mine, Eureka Mining District, San Juan County, Colorado: Geochemistry of gold and basemetal ore deposition in a volcanic environment: Econ. Geol., v. 72, p. 1285-1320.

Cunningham, Charles C., and Hall, Robert B., 1976, Field and Laboratory tests for the detection of alunite and the determination of atomic percent potassium: Econ. Geol., v. 71, p. 1596-1598.

Doe, B.R., Steven, T.A., Delevaux, M.H., Stacey, J.S. Depiven, P.W., and Fisher, F.S., 1979, Genesis of ore deposits in the San Juan volcanic field, southwestern Colorado--lead isotope evidence Econ. Geol., v. 74, no. 1, p. 1-26.

Drew, D.P., and Cohen, J.M., 1980, Geomorphology and sediments of Aillwee Cave, County Claire, Ireland: Proc. Univ. Bristol Spelaeol. Soc., v. 15, no. 3, p. 117-240.

Drummond, Segal. E.J., 1981, Boiling and mixing of hydrothermal fluids: chemical effects of mineral precipitation: Dept. of Geosciences, Pennsylvania State Univ., Unpublished Ph.D. thesis, 380 p.

Gary, Margaret, McAfee, Robert, Jr., and Wolf, Carol, L. (eds.), 1972, Glossary of Geology: Washington, D. C., American Geological Institute, 805 p.

Hemley, J.J., Hostetler, P.B., Gude, A.J., and Mountjoy, W.T., 1969, Some stability relations of alunite: Econ. Geol., v. 64, p. 599-612.

Henley, R.W., 1973, Solubility of gold in hydrothermal chloride solutions: Chem. Geology, v. 11, p. 73-87.

Henley, R.W., and Ellis, A.J., 1983, Geothermal systems ancient and modern: a geochemical review: Earth-Science Reviews, v. 19, p. 1-50.

Hon, Ken, Lipman, P.W., and Mehnert, H.H., 1983, The Lake City caldera, western San Juan Mountain, Colorado: Geol. Soc. America Abstracts with Programs v. 15, no. 5, p. 389.

Hon, Ken, Ludwig, K.R., Simmons, K.R., Slack, J.F., and Grauch, R.I., 1985, U-Pb Isochron Age and Pb Isotope Systematics of the Golden Fleece vein--Implications for the Relationship of Mineralization to the Lake City Caldera, Western San Juan Mountains, Colorado: Economic Geology, v. 80, p. 410-417.

Irving, J.D., and Bancroft, H., 1911, Geology and ore deposits near Lake City, Colorado: U.S. Geol. Survey Bull. 478, 128 p.

Joseph, Dominique, and Touray, Jean-Claude, 1974, Underground sediments in a fluorite vein at Maine (Cordesse 71-France): Econ. Geol., v. 69, p. 545-556.

Kalliokoski, J., and Billings, Patty, 1982, Sediment-filled veins of the Golden Wonder Mine, Lake City, Colorado: Geol. Soc. America Abstracts, v. 14, no. 7, p. 524.

Kendall, D.L., 1960, Ore deposits and sedimentary features, Jefferson City Mine, Tennessee: Econ. Geol., v. 55, p. 985-1003.

Kesler, S.E., Russell, N., Seaward, M., Rivera, J., McCurdy, K., Cumming, G.L., and Sutter, J.F., 1981, Geology and geochemistry of sulfide mineralization underlying the Pueblo Viejo gold-silver oxide deposit, Dominican Republic: Econ. Geol., v. 76, p. 1096-1117.

Knight, Jerry E., 1977, A thermochemical study of alunite, enargite, luzonite, and tennantite deposits: Econ. Geol., v. 72, p. 1321-1336.

Lindgren, Waldemar, 1933, Mineral deposits: New York, N. Y., McGraw Hill, Inc., 4th edition, 929 p.

Lipman, P.W., 1976, Geologic map of the Lake City caldera area, western San Juan Mountains, southwestern Colorado: U.S. Geol. Survey Misc. Inv. Map I-962, scale 1:48,000.

Lipman, P.W., Steven, T.A., Luedke, R.G., and Burbank, W.S., 1973. Revised volcanic history of the San Juan Uncompahgre, Silverton, and Lake City calderas in the western San Juan Mountains, Colorado: U.S. Geol. Survey Jour. Research, v. 1, no. 6, p. 627-642.

Lipman, P.W., Fisher, F.S., Mehnert, H.H., Naeser, C.W., Luedke, R.G., and Steven, T.A., 1976, Multiple ages of mid-Tertiary mineralization and alteration in western San Juan Mountains, Colorado: Econ. Geol., v. 71, p. 571-588.

Lloyd, E.F., 1959, The hot springs and hydrothermal eruptions of Waistapn: New Zealand Journal Geol. and Geophys., v. 2, p. 141-176.

Lovering, T.G., 1958, Temperature and depth of formation of sulfide ore deposits of Gilman, Colorado: Econ. Geol., v. 53, p. 689-707.

Luce, Frederick, D., Tuttle, Catherine L., and Skinner, Brian J., 1977, Studies of sulfosalts of copper: V. phases and phase relations in the system Cu-Sb-As-S between 350° and 500°C: Econ. Geol., v. 72, p. 271-289.

Meyer, C., and Hemley, J.J., 1967, Wallrock alteration, in Barnes, H.L., ed., Geochemistry of hydrothermal ore deposits: New York, Holt, Rinehart and Winston, p. 166-235.

Monroe, W.H., 1973, A possible origin of clay fill in caves: Sixth International Congress of Speleology Proceedings, Olomouc, Czechoslovakia, 1973, p. 509-512.

Reynolds, Richard L., and Goldhaber, Martin B., 1983, Iron disulfide minerals and the genesis of roll-type uranium deposits: Econ. Geol., v. 78, p. 105-120.

Romberger, S.B., 1982, Transport and deposition of gold in hydrothermal systems at temperatures up to 300°C: Geol. Soc. America Abstracts, v. 7, p. 602.

Romberger, 1986, Ore deposits #9. Disseminated gold deposits: Geoscience Canada, v. 13, p. 23-31.

Schoen, R., White, D.E., and Hemley, J.J., 1974, Argillization by decending acid at Steamboat Springs, Nevada: Clays and Clay Minerals, v. 22, p. 1-22.

Seward, T.M., 1973, Thio complexes of gold and the transport of gold in high temperature ore solutions: Geochim. et Cosmochim. Acta, v. 37, p. 379-399.

Sigvaldason, G.E., and White, D.E., 1962, Hydrothermal alteration in drill holes GS-5 and GS-7, Steamboat Springs, Nevada: U.S. Geological Survey Professional Paper 450-D, p. D113-117.

Sillitoe, R.H.,1985, Ore-related breccias in volcanoplutonic areas: Economic Geology, v. 80, p. 1467-1514.

Sillitoe, R.H., Grauberger, G.L., and Elliott, J.E., 1985, A diatreme-hosted gold deposit at Montana Tunnels, Montana: Economic Geology, v. 80, p. 1707-1721.

Slack, John F., 1976, Hypogene zoning and multistage vein mineralization in the Lake City Area, western San Juan Mountains, Colorado: Stanford Univ., Stanford, CA, Unpubl. Ph.D. thesis, 327 p.

_____1980, Multistage vein ores of the Lake City District, western San Juan Mountains, Colorado: Econ. Geol., v. 75, p. 963-991.

Sohnge, P.G., 1963, Genetic problems of pipe deposits in South Africa: Geol. Society South Africa Trans., v. 66, p. 19-22.

Strachan, Donald G., Pettit, Paul M., and Reid, Richard F., 1982, The geology of the Borealis gold deposit, Mineral County, Nevada: Geol. Soc. America Abstracts with Programs, v. 14, p. 625.

Vaughan, David J., and Craig, James R., 1978, Mineral chemistry of metal sulfides: Cambridge University Press, Cambridge, MA, 493 p.

White, D.E., 1955, Thermal springs and epithermal deposits, in Bateman, A.M., ed.: Econ. Geol. Fiftieth Anniversary Vol, p. 99-154.

_____1981, Active geothermal systems and hydrothermal ore deposits: Econ. Geol. Seventy-Fifth Anniversary Vol., p. 392-423.

White, D.E., Muffler, L.S.P., and Truesdell, A.H., 1971, Vapor-dominated hydrothermal systems compared with hot-water systems: Econ. Geol., v. 66, p. 75-97.

White, Elizabeth L., and White, William B., 1968, Dynamics of sediment transport in limestone caves: National Speleological Soc., Bulletin, v. 30, p. 115-129.

FIGURE CAPTIONS

Figure 1. Generalized geologic map of the Lake City area, Colorado, showing distribution of veins (from Hon and others, 1985). Numbered localities: (1) Golden Wonder Mine; (2) Golden Fleece Mine and vein; (3) Ute-Ulay Mine.

Figure 2. Schematic west-east cross section, Golden Wonder Mine, showing extent of mine workings, and stratigraphy from Lipman (1976).

Figure 3. West-east cross section, Golden Wonder Mine, showing orientation of flow foliation and distribution of bedded rhyolite breccia (pyroclastic apron deposit) in the rhyolite of Volcanics of Uncompahgre Peak (Lipman and others, 1976).

Figure 4. Plan-view map of third level showing structure and wallrock alteration.

Figure 5. Plan-view map of east end of sixth level. The east end is shown diagramatically in figure 13.

Figure 6. Plan-view map of fourth level and sublevel showing structure, alteration, and mineralization.

Figure 7. Thin section of flow-banded felsic volcanic rock, devitrified and subsequently completely altered to quartz and kaolinite. Equant quartz phenocryst (lower right), embayed quartz phenocryst (upper right), pyrite (black). Unpolarized; length of field 3 mm.

Figure 8. Porphyritic rhyolite, probably welded crystal tuff. Embayed quartz phenocryst (center) contains devitrified glass inclusions. Compare with quartz clasts, fig. 18. Three feldspar phenocrysts (equant grains) are altered completely to kaolinite. Matrix contains abundant secondary quartz and kaolinite, some selectively replacing the pyroclastic matrix. Partly crossed polars; length of field 3 mm.

Figure 9. Breccias and sediments filling an open fissure that follows a stair-step-like textural contact in rhyolite (4, 5, 6, in figure 11). The lowest filling is unbedded chert-pyrite breccia. This and the footwall rhyolite are overlain by bedded quartzose sandstone. The succeeding overlying sediment grades upward into unbedded alunite. The uppermost body is brecciated alunite, in clay-altered rhyolite, with abrupt contact against silicified rhyolite. Winze, 23 to 27 m (88 feet) below third level, view northeast along strike.

Figure 10. Fissure-fill of chert-pyrite breccia and cross-bedded quartzose sandstone, viewed normal to strike of vein (4 and 5, fig. 11); hanging wall rhyolite (top), footwall rhyolite (bottom). Footwall overlain by unbedded chert breccia (right). This and rhyolite faulted, and sandstone deposited against fault surface. Sediments, all well cemented, range from siltstone to conglomerate. Winze, 27 to 28 m (88 to 92 ft) below third level.

Figure 11. Diagram showing observed and inferred relationships among veins, sediments, alteration, and mineralization in the Golden Wonder Mine: (1) quartz-pyrite-marcasite vein; (2) brecciated vein (3) "tetrahedrite" crusts on cavity wall; (4) unbedded chert-pyrite breccia; (5) bedded quartzose sediment and bedded breccia; (6) sedimentary alunite; (7) fragments and interlayers of colloform sulfides. Not to scale.

Figure 12. Symmetrical colloform-banded vein of radially grown pyrite, terminating in a thin layer of marcasite in rhyolite wallrock. In lower left is an outer zone of quartz-kaolinite (1); in the inner quartz-rich zone, disseminated pyrite increases in abundance toward the vein (2). The center of the vein is filled with vein-brecciation-stage alunite with a transported fragment of pyrite (3). Fractures with minor offset that cross colloform pyrite also denote vein brecciation. Sixth level; scale in centimeters.

Figure 13. Diagram of 10 m (30 ft) portion of vein, east end, sixth level (see figure 5), showing how quartz-pyrite-marcasite vein (1) cuts breccia dike and terminates in vein breccia (2) in which vein fragments occur in an alunite matrix. Along the east end of the vein, wall rocks are alunitized, and part of the vein and alunitized wall rocks are contorted (3); (4) location of figure 12; not to scale.

Figure 14. Silicified porphyritic rhyolite (left); former cavity (right), cavity wall covered by a film of "tetrahedrite". Cavity-filling sediment is quartz sandstone at bottom, finer grained and more cemented near the top. Scours along base of some beds. Dark pigmentation is sulfide. Beds offset against wallrock, possibly caused by compaction or drag. White areas are kaolinite. Third-level dump. Specimen is about 7 cm long.

Figure 15. Unbedded chert-pyrite breccia with clasts of chert, silicified rhyolite, and sulfide (dark). Matrix in silica-cemented breccia. Third-level dump: Specimen is 10 cm long.

Figure 16. Two layers of fine-grained crossbedded sandstone, both overlain by finer grained more kaolinitic quartzose sediment. White spots are kaolinite. Porous zone above lowest sand layer (lower right) may be hot-spring sinter. Crossbeds enhanced by dark sulfides. Third-level dump; scale in centimeters.

Figure 17. At bottom, two beds of variously silicified possible chert breccia or hot-spring sinter overlain by 1 cm layer of chert-pyrite breccia (center). The upper coarse sandstone rests on a finer grained pyritized and partly eroded layer of sandstone. In the upper bed, the 1 mm quartz grains are phenocrysts probably liberated from lower in the volcanic section. Third-level dump; specimen is 9 cm high.

Figure 18. Thin section of quartzose sandstone with large quartz clasts, probably derived from quartz phenocrysts, in a fine-grained matrix of clastic and cherty quartz, kaolinite, and alunite. The deep embayment in quartz (upper right), originally probably filled with glass, is now kaolinite. Nicols partly crossed; width of field 3 mm.

Figure 19. Bedded kaolinite and alunite, larger kaolinite clots probably denote top of bed. A chemical sediment. Third-level dump; specimen is 9 cm high.

Figure 20. At base a coarse grained chert-cemented sediment with secondary porosity, crossed by a lighter colored zone of sinter(?). Above this (lower left) a well-laminated sediment overlying an irregular floor, and overlain by a sediment with a rip-up chip (white center right) of alunite-cemented quartz siltstone. Overlying material highly porous, origin uncertain. Third-level dump; specimen is 6 cm high

Figure 21. Polished section showing sulfide grains along crossbeds in coarse-grained quartz sandstone. Larger equant grains are pyrite, small irregular ones are chalcopyrite-pyrite clusters. Largest pyrite grains are 0.1 mm in diameter.

Figure 22. Cavity filling of fine-grained pyrite-chalcopyrite (bottom), overgrown by 4 mm galena layer (shiny faces) and a thin overlying crust of pyrite. These minerals buried under bedded alunite cut by growth-type compaction faults. Third-level dump; scale in centimeters.

Figure 23. Possible synsedimentary alteration or soft-sediment deformation features in sedimentary alunite. Older darker brown alunite with disrupted clasts of sulfides (bottom); this is cut by younger lighter brown alunite. Third-level dump; height of specimen 7 cm.

Figure 24. Clots of white alunite (perhaps derived from kaolinite by alteration) in darker brown alunite, both cut by very fine veinlets of alunite. White clots flattened in the plane of photograph denote soft-sediment deformation. Third-level dump; scale in centimeters.

Figure 25. Polished section of inclusion-free chalcopyrite (left), rimmed by scattered small, irregular clusters of colloform covellite (gray) and a 0.1 mm layer of chalopyrite with alunite inclusions (dark specks). Abundant small clusters of covellite (gray) along large-grain periphery, coated by thin film of pyrite (white). Polygonal grains of chalcopyrite and of pyrite, and dendritic grains of pyrites, in alunite matrix (center). Width of field 1 mm.

Figure 26. Polished section of galena (white, bladed, center), altered parallel to cleavage to anglesite (gray, few inclusions) in a matrix of alunite (with more black specks). Microcolloform pyrite crusts outline two anglesite pseudomorphs of galena. The spherical and dendritic crystals in alunite are pyrite.

Figure 27. Polished section of sylvanite (1, polysynthetically twinned, whitest), native tellurium (2, softer, grey mineral), and melonite (3, fine-grained aggregates, left center and right), with patches of alunite matrix. Oil immersion, nicols partly crossed.

Figure 28. Polished section, showing microcrystalline and sketal forms of pyrite, thought to represent disequilibrium precipitation, in an alunite matrix. No marcasite identified.

Figure 29. Round grains of sphalerite with minor wurtzite (not visible), containing tabular crystals of alunite, in an alunite matrix. Dark spots are pits. The crystallization of alunite overlapped that of sphalerite. Width of field 6 mm.

Figure 30. Chalcopyrite (light gray) with alunite (dark grey). Dark areas are pits. The curved chalcopyrite surfaces denote either a rapid colloform growth from a saturated solution, or the greater surface energy of chalcopyrite as it grew in alunite mud. Width of field 1.2 mm.

Figure 31. Proposed geological setting of the Golden Wonder Mine in a hot-spring depositional model (modified from Berger and Eimon, 1982).

Figure 32. Isothermal log fO_2-fS_2 diagram at 250°C and 1 atm pressure showing possible chemical environments of mineral deposition; ΣS= 0.01 m; K+ = 0.05 m (modified from Slack, 1980 and Kesler and others, 1981). Point a, position of early quartz-pyrite-marcasite mineralization associated with quartz-kaolinite wallrocks; b, late-stage alunite-pyrite deposition, also chalcopyrite-pyrite-alunite-kaolinite deposition in quartzose sandstones.

Figure 33. Isothermal log aO_2-pH diagram, at 250°C and 1 atm pressure. a. shows solubility of gold; ΣS - 0.01 m; ΣCl = 0.1 m; ΣC = 0.1 m; Σ Au = 10^{-9} m (from Barnes, 1982). b. shows stability fields of important iron-bearing minerals and of alunite, (alunite modified from Kesler and others, 1981). If the chemical system is at point a (also fig. 32, point a) and shifts to b, gold solubility decreases by one order of magnitude and alunite begins to form.

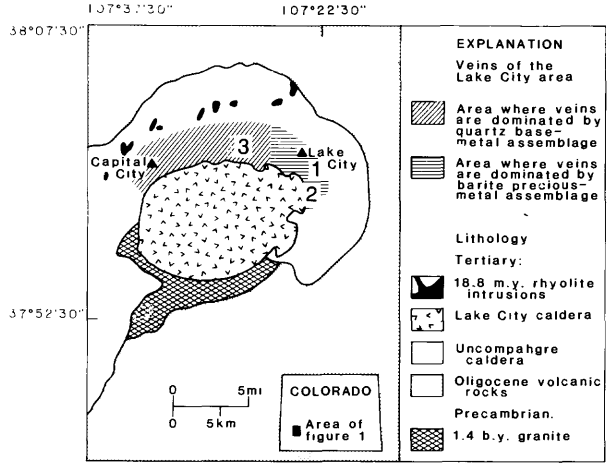

Figure 1

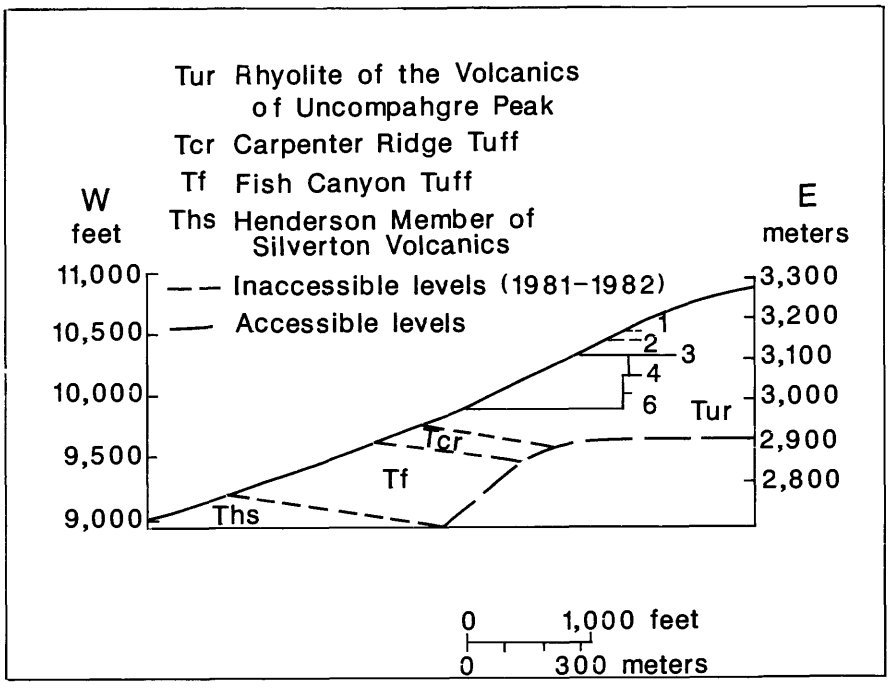

Figure 2

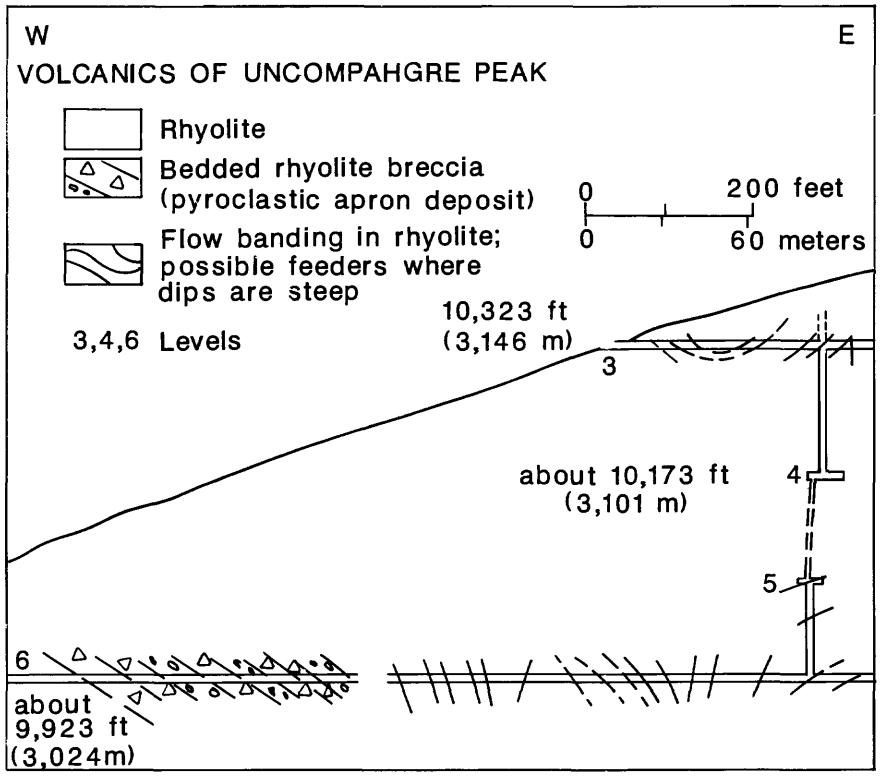
W
E
VOLCANICS OF UNCOMPAHGRE PEAK
Rhyolite
Bedded rhyolite breccia
(pyroclastic apron deposit)
Flow banding in rhyolite;
possible feeders where
dips are steep
3,4,6 Levels
0
200 feet
0
60 meters
10,323 ft
(3,146 m)
3
about 10,173 ft
(3,101 m)
4
5
6
about
9,923 ft
(3,024m)

Figure 3

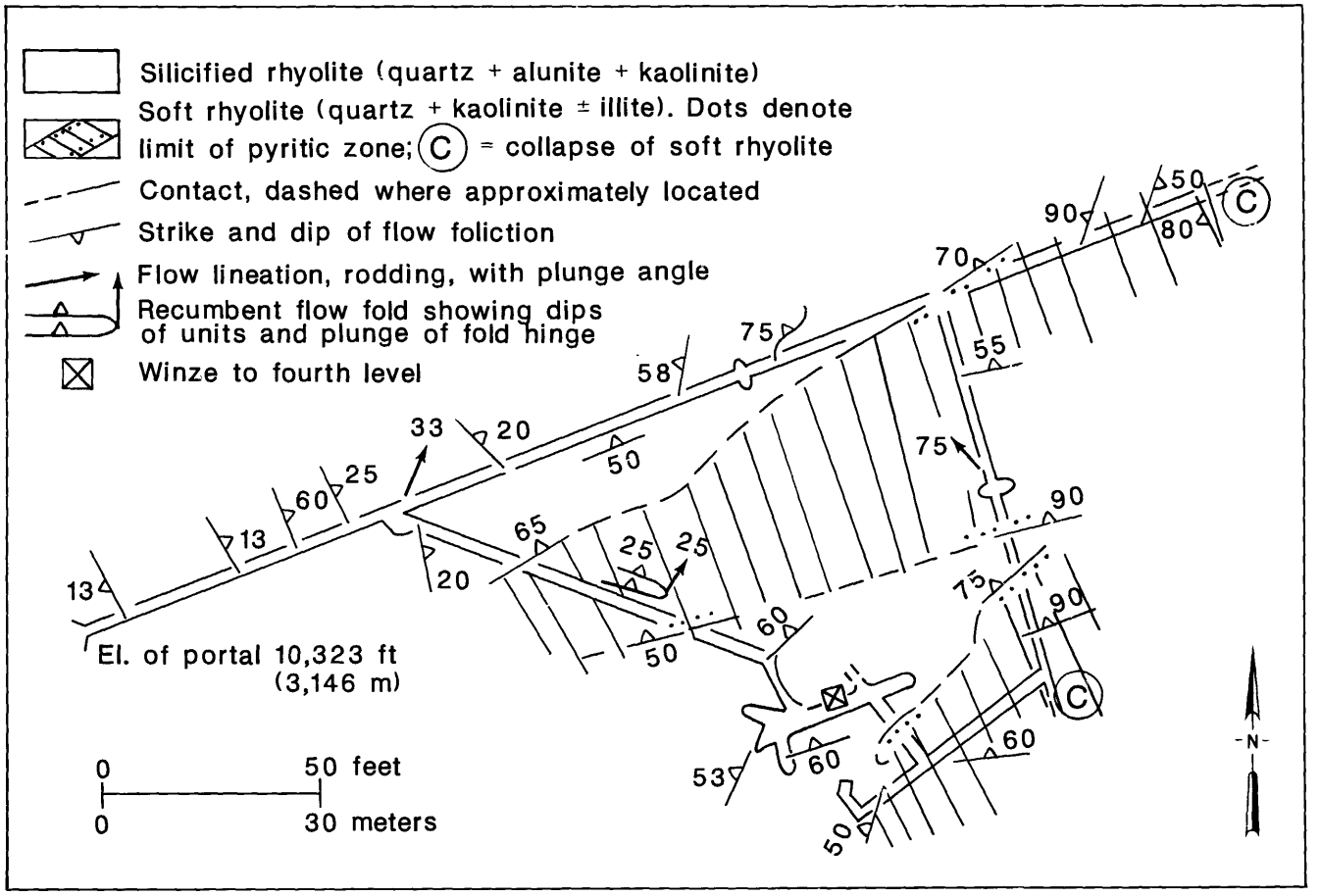
Silicified rhyolite (quartz + alunite + kaolinite)
Soft rhyolite (quartz + kaolinite ± illite). Dots denote limit of pyritic zone; (C) = collapse of soft rhyolite
Contact, dashed where approximately located
Strike and dip of flow foliction
Flow lineation, rodding, with plunge angle
Recumbent flow fold showing dips of units and plunge of fold hinge
Winze to fourth level
El. of portal 10,323 ft (3,146 m)
0 50 feet
0 30 meters
N

Figure 4

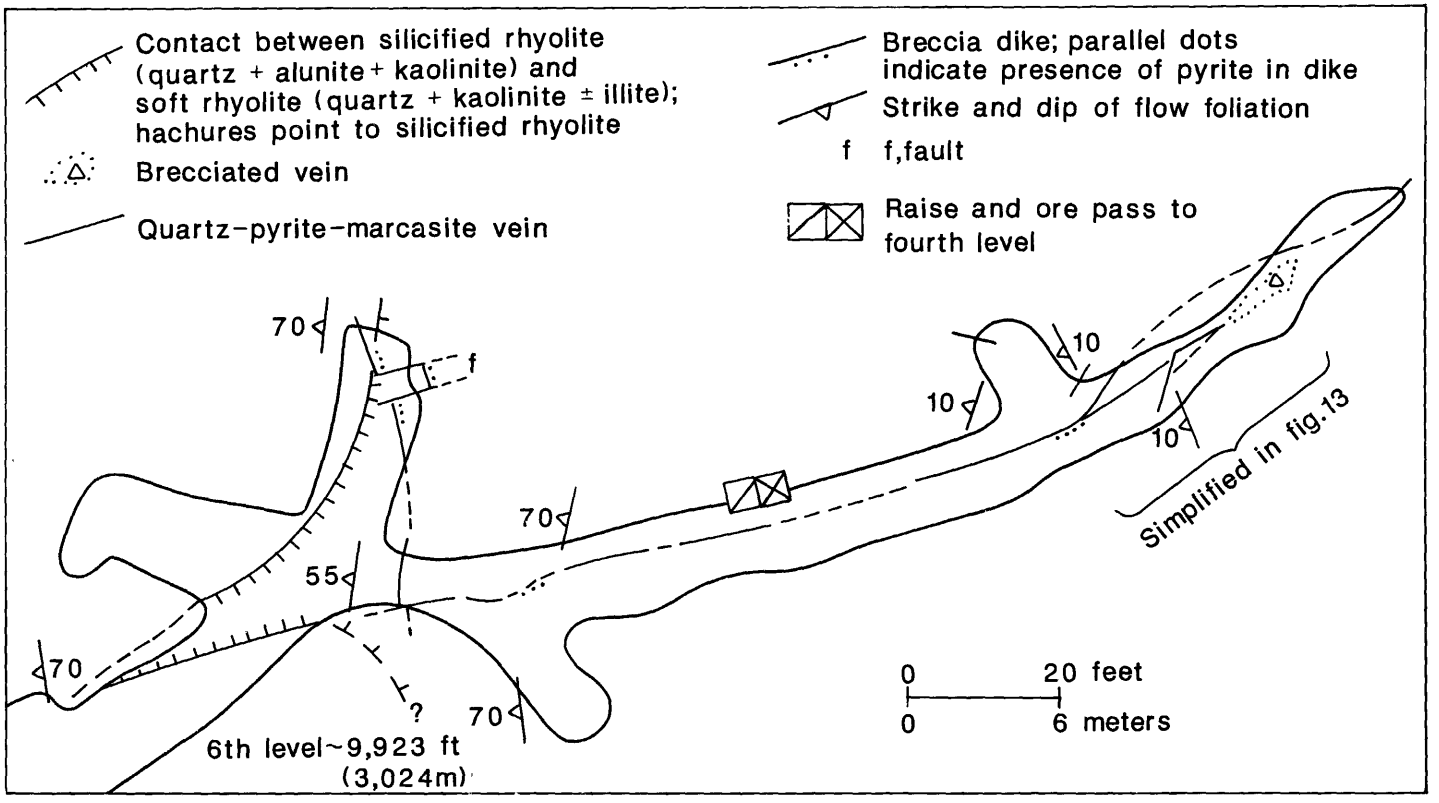
Contact between silicified rhyolite (quartz + alunite + kaolinite) and soft rhyolite (quartz + kaolinite ± illite); hachures point to silicified rhyolite
Brecciated vein
Quartz-pyrite-marcasite vein
Breccia dike; parallel dots indicate presence of pyrite in dike
Strike and dip of flow foliation
f f,fault
Raise and ore pass to fourth level
70
f
10
10
10
70
55
70
70
?
Simplified in fig.13
0 20 feet
0 6 meters
6th level~9,923 ft
(3,024m)

Figure 5

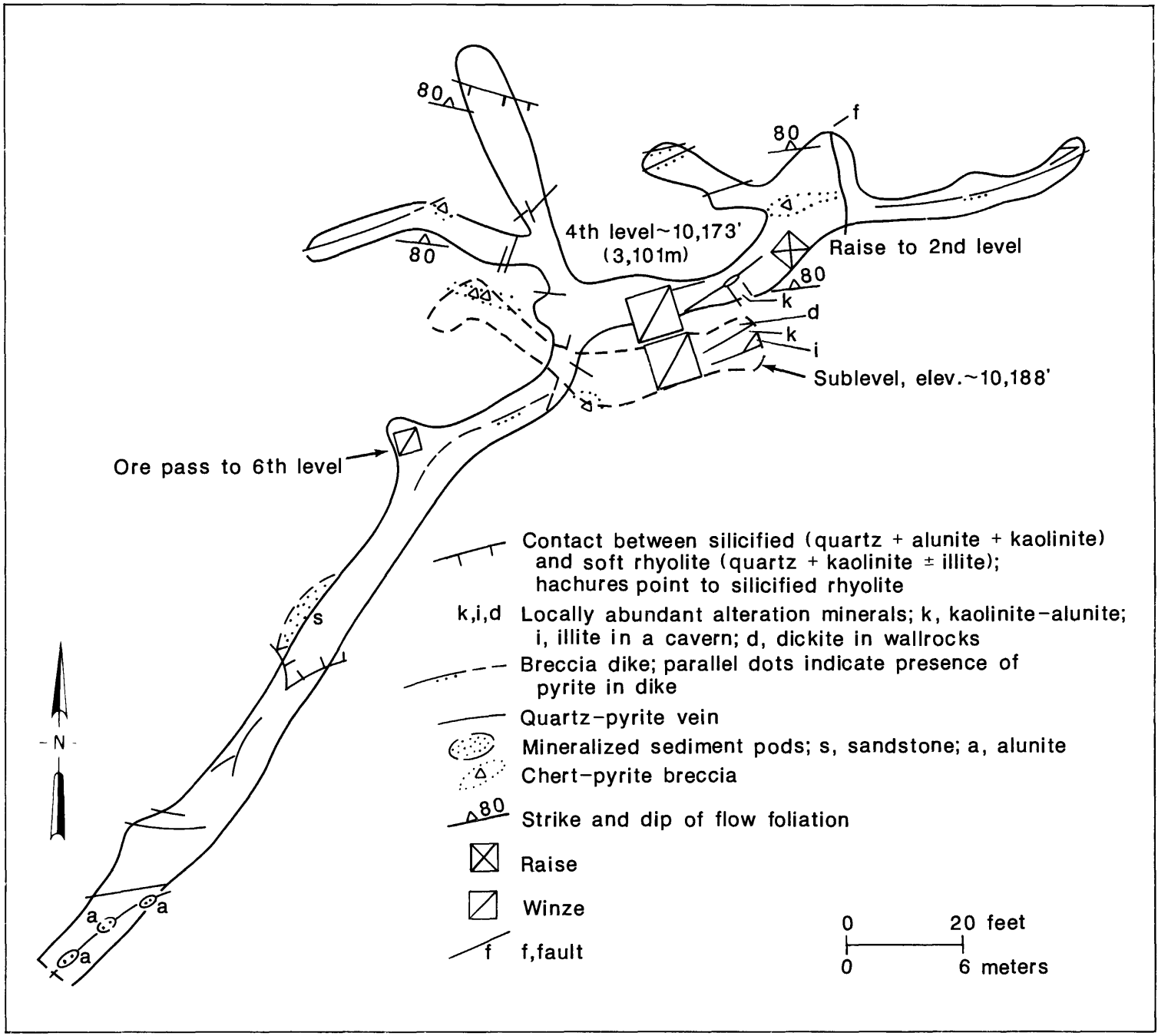
80
80
80
f
4th level~10,173'
(3,101m)
Raise to 2nd level
80
k
d
k
i
Sublevel, elev.~10,188'
Ore pass to 6th level
s
N
a
a
a
Contact between silicified (quartz + alunite + kaolinite) and soft rhyolite (quartz + kaolinite ± illite); hachures point to silicified rhyolite
k,i,d Locally abundant alteration minerals; k, kaolinite-alunite; i, illite in a cavern; d, dickite in wallrocks
Breccia dike; parallel dots indicate presence of pyrite in dike
Quartz-pyrite vein
Mineralized sediment pods; s, sandstone; a, alunite
Chert-pyrite breccia
80 Strike and dip of flow foliation
Raise
Winze
f f,fault
0 20 feet
0 6 meters

Figure 6

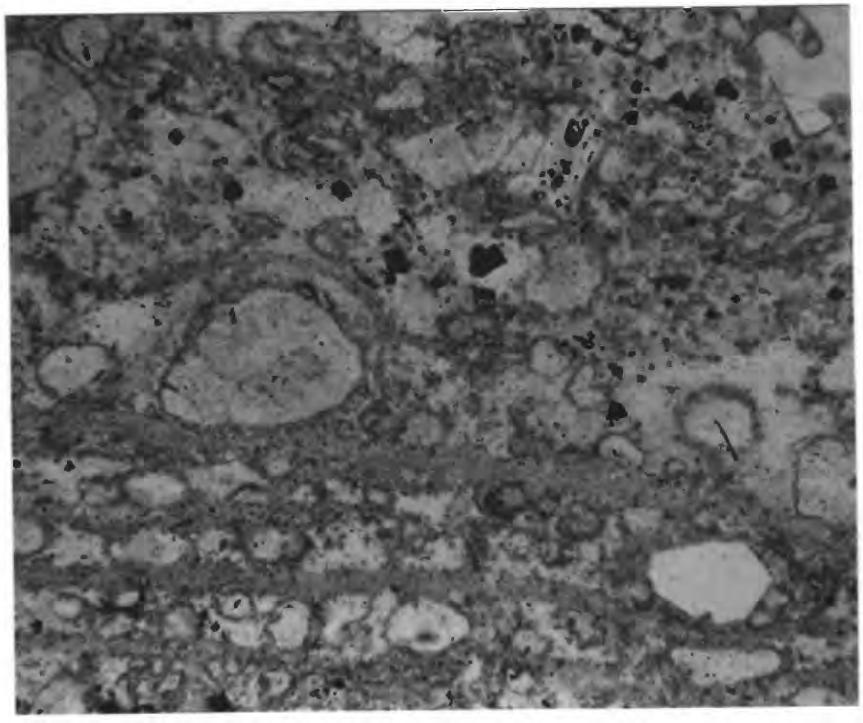

Figure 7

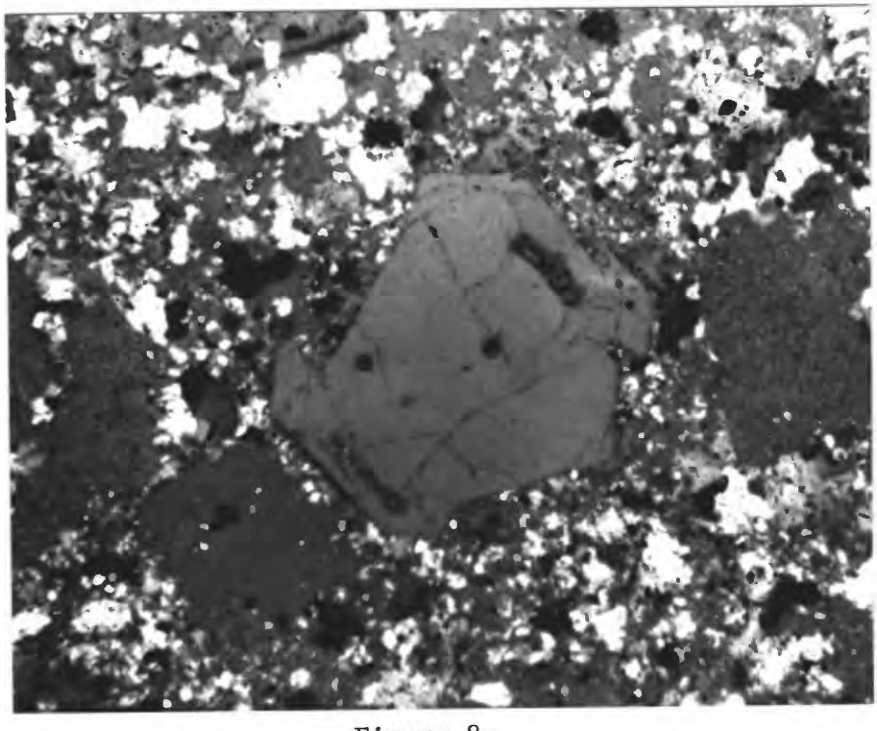

Figure 8

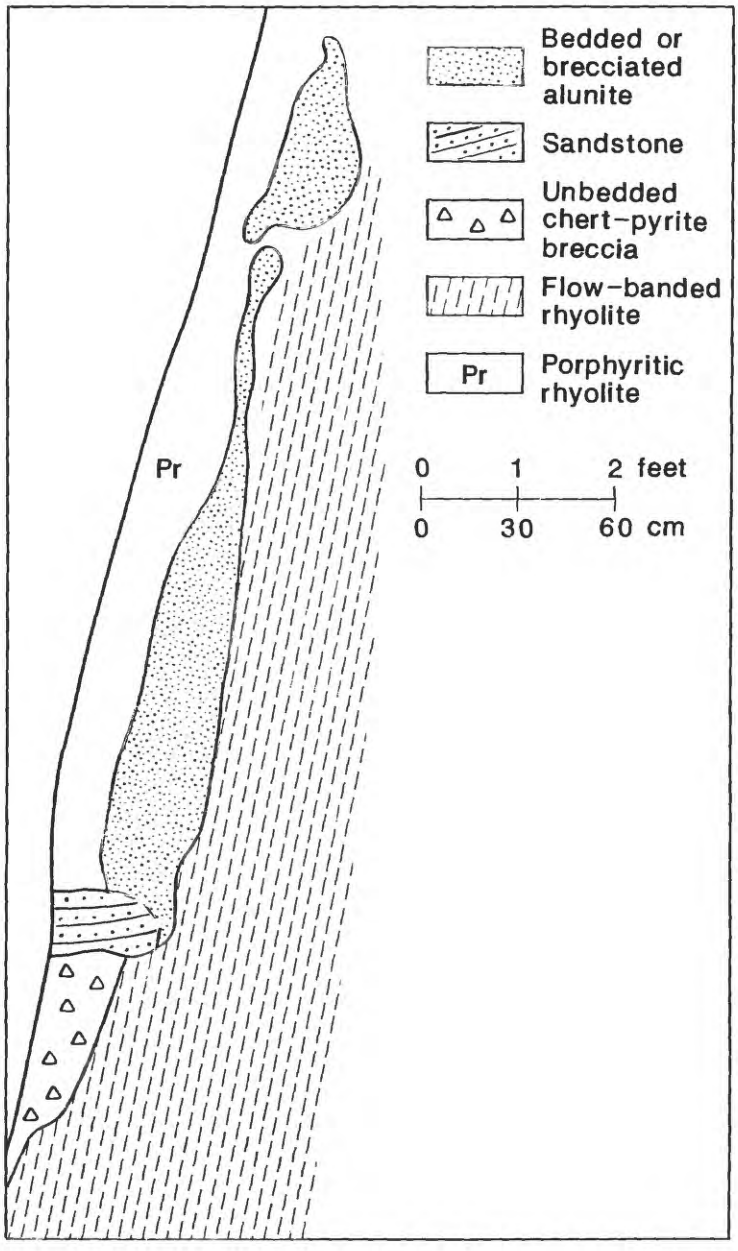
Bedded or brecciated alunite
Sandstone
Unbedded chert–pyrite breccia
Flow–banded rhyolite
Pr
Porphyritic rhyolite
Pr
0 1 2 feet
0 30 60 cm

Figure 9

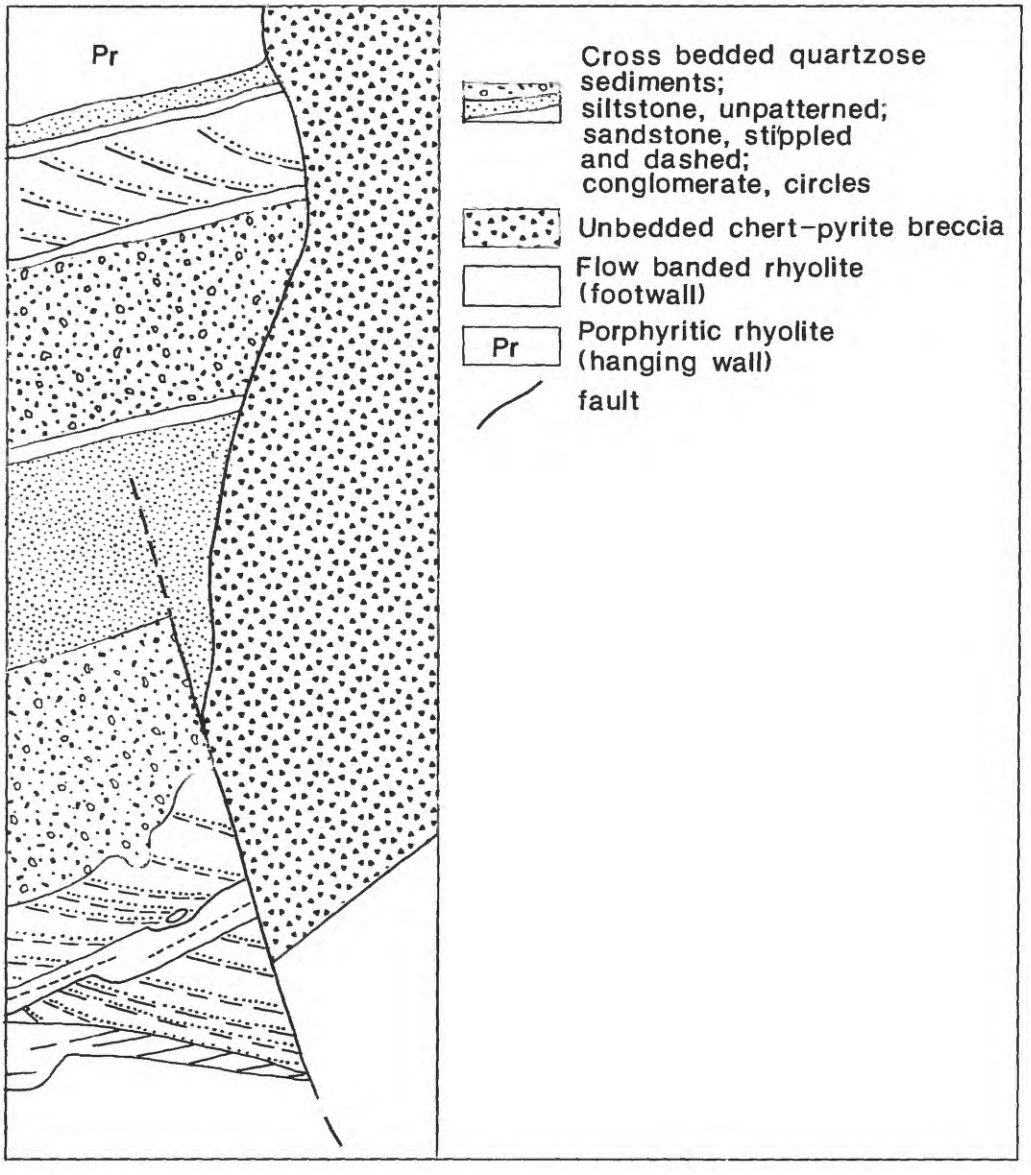
Pr
Cross bedded quartzose sediments;
siltstone, unpatterned;
sandstone, stippled and dashed;
conglomerate, circles
Unbedded chert–pyrite breccia
Flow banded rhyolite (footwall)
Pr
Porphyritic rhyolite (hanging wall)
fault

Figure 10

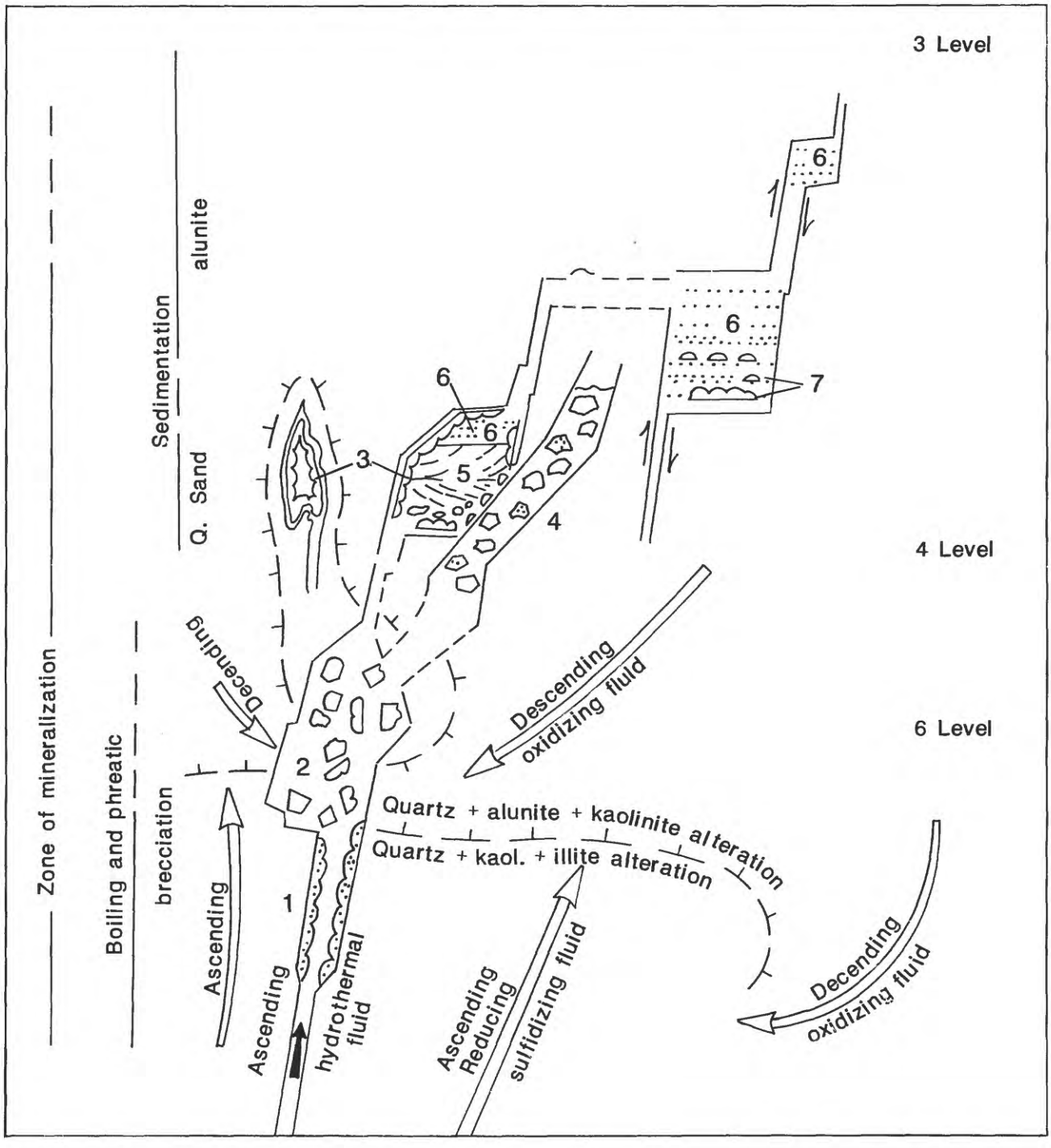
3 Level
4 Level
6 Level
Zone of mineralization
Boiling and phreatic
brecciation
Sedimentation
alunite
Q. Sand
Ascending
Decending
Descending
oxidizing fluid
Quartz + alunite + kaolinite alteration
Quartz + kaol. + illite alteration
Ascending
hydrothermal
fluid
Ascending
Reducing
sulfidizing fluid
Decending
oxidizing fluid
1
2
3
4
5
6
7

Figure 11

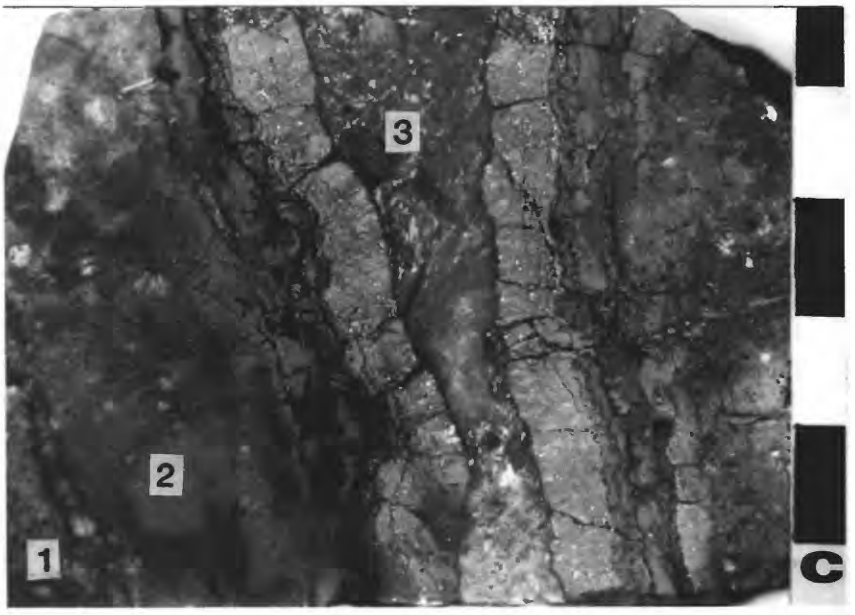

Figure 12

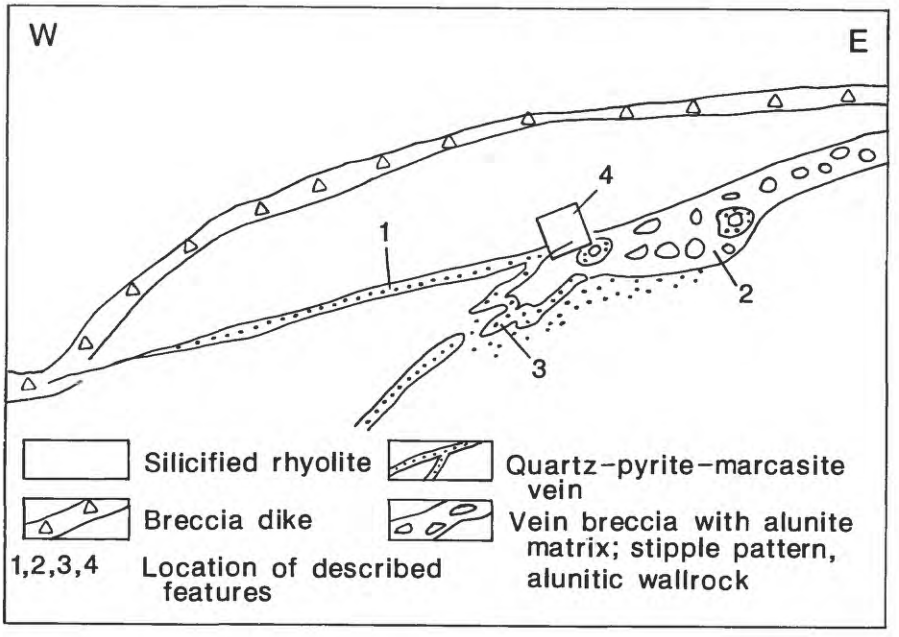

Figure 13

Figure 14

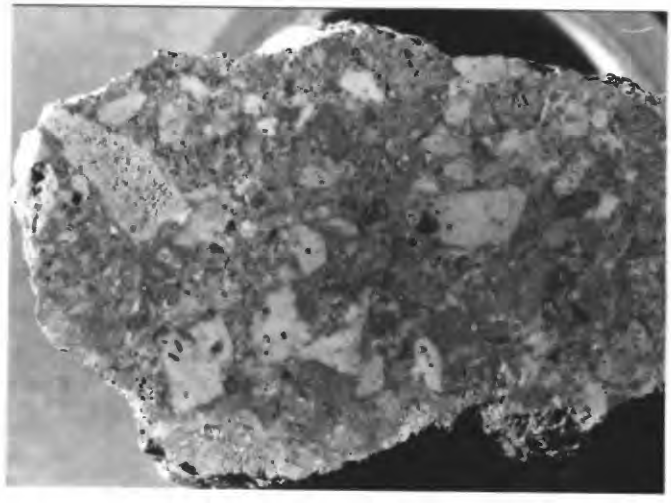

Figure 15

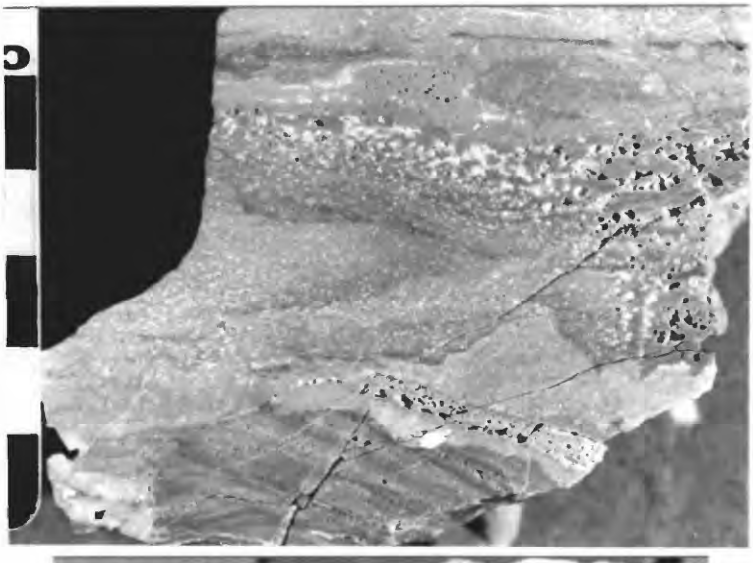

Figure 16

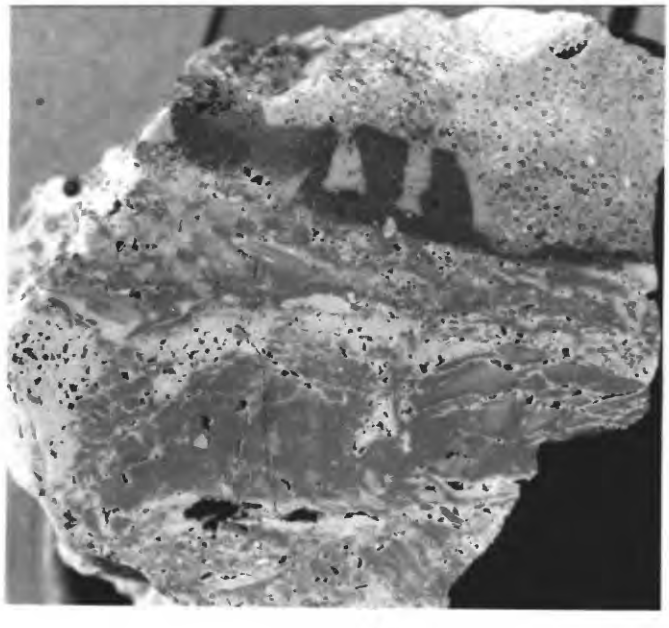

Figure 17

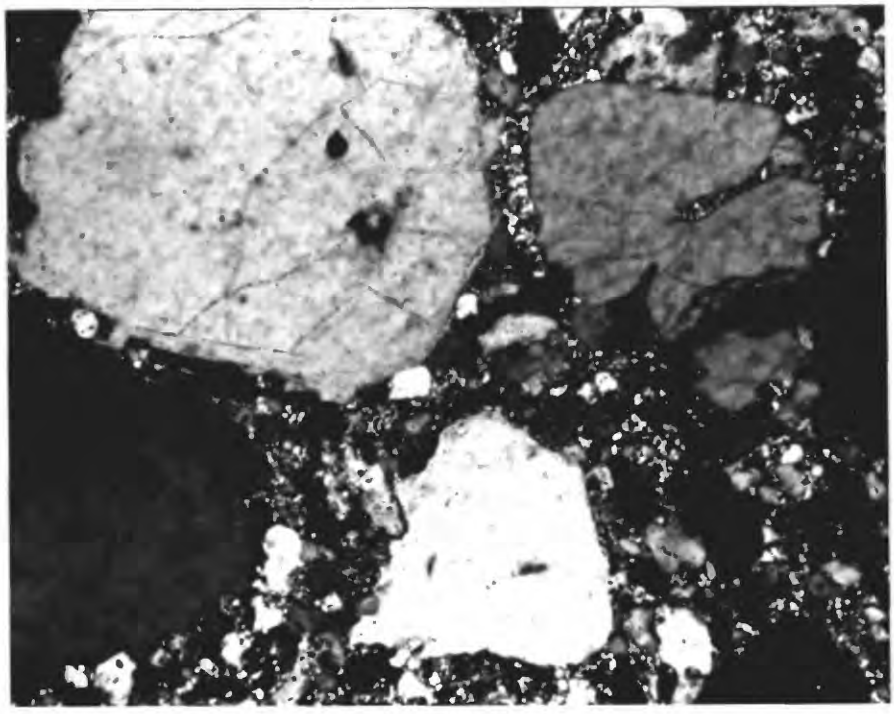

Figure 18

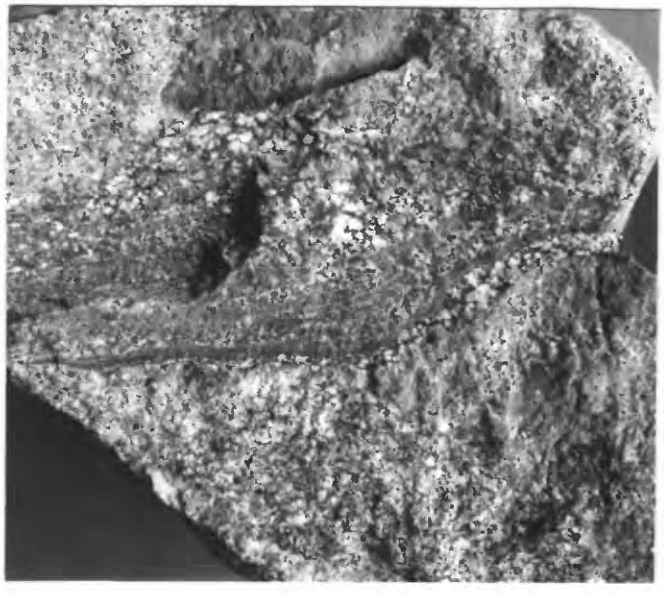

Figure 19

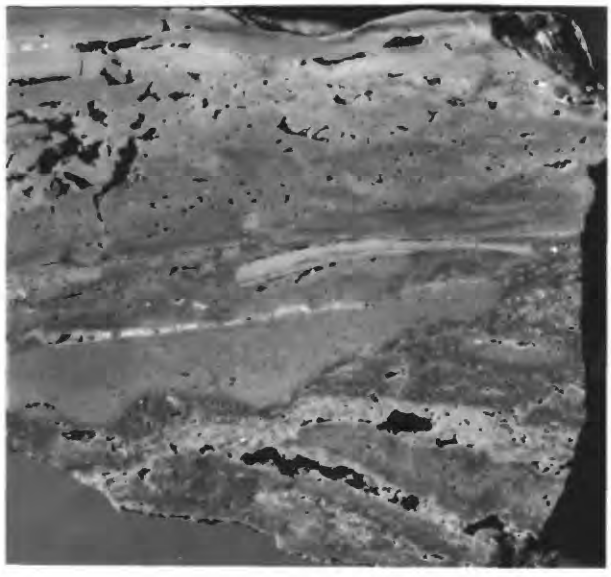

Figure 20

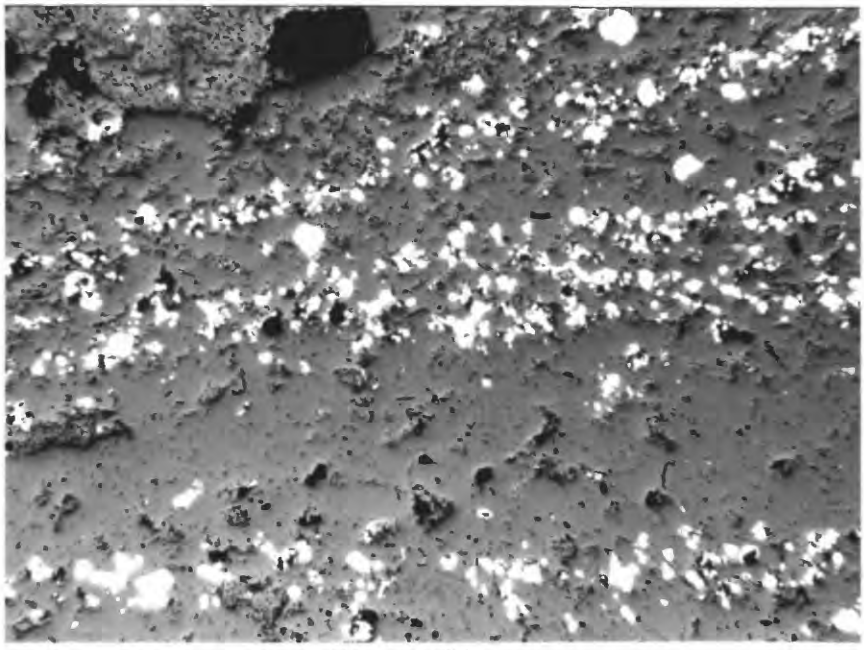

Figure 21

Figure 22

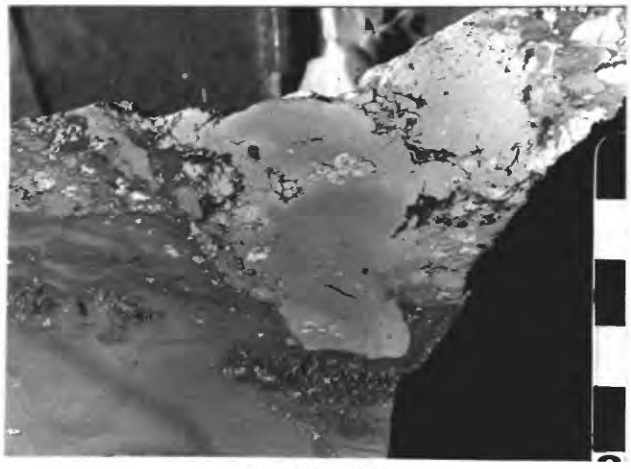

Figure 23

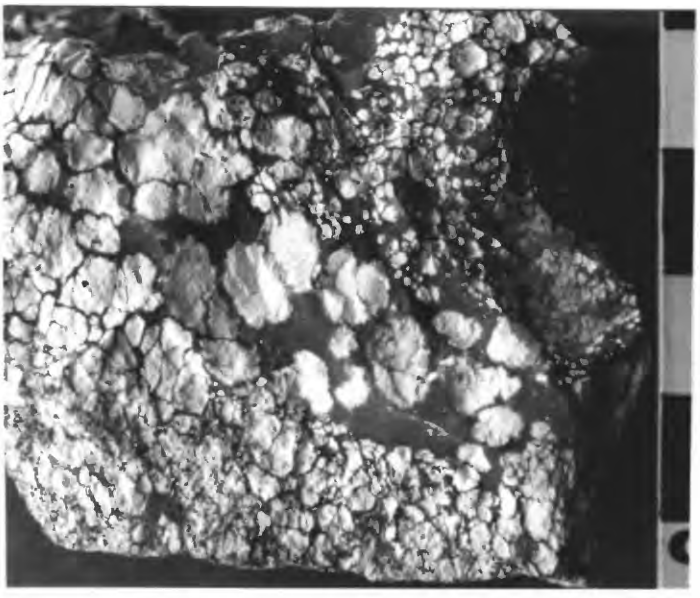

Figure 24

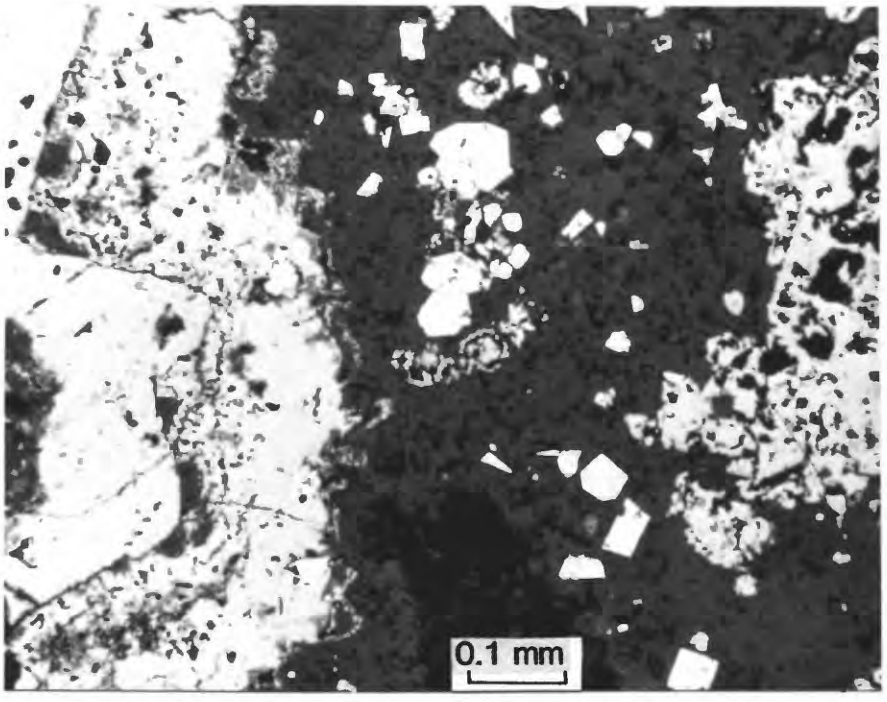

Figure 25

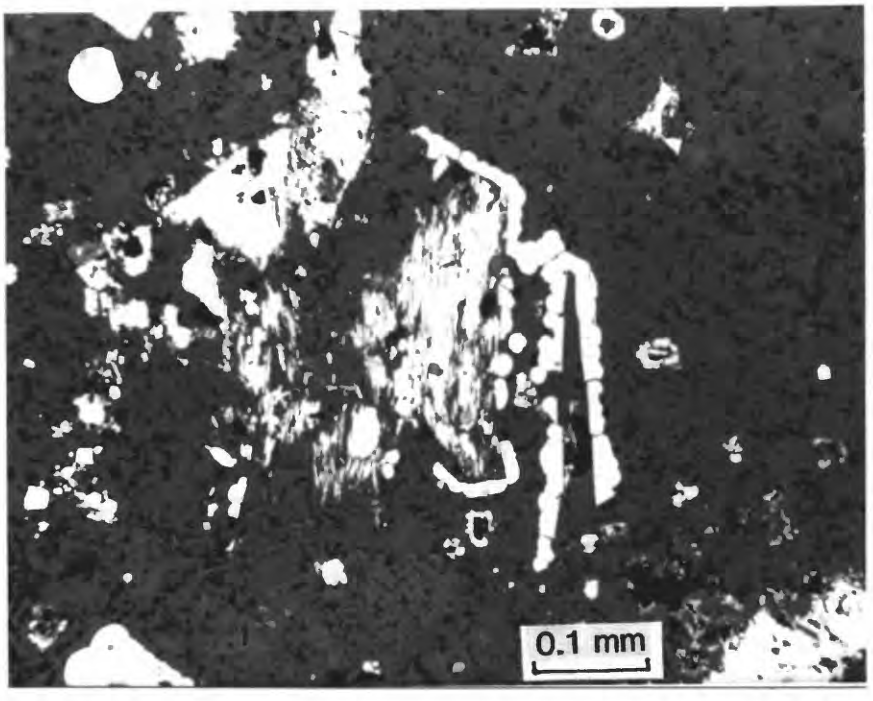

Figure 26

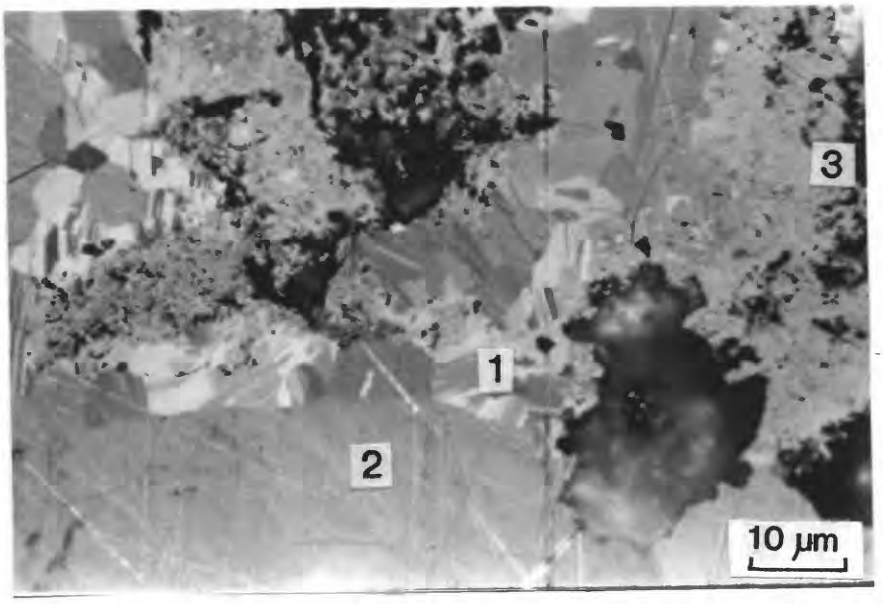

Figure 27

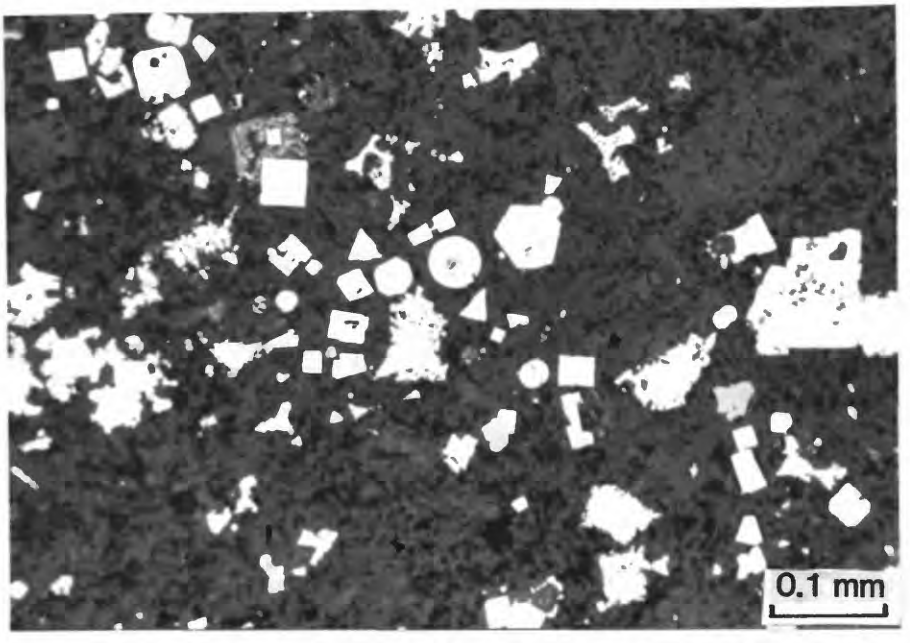

Figure 28

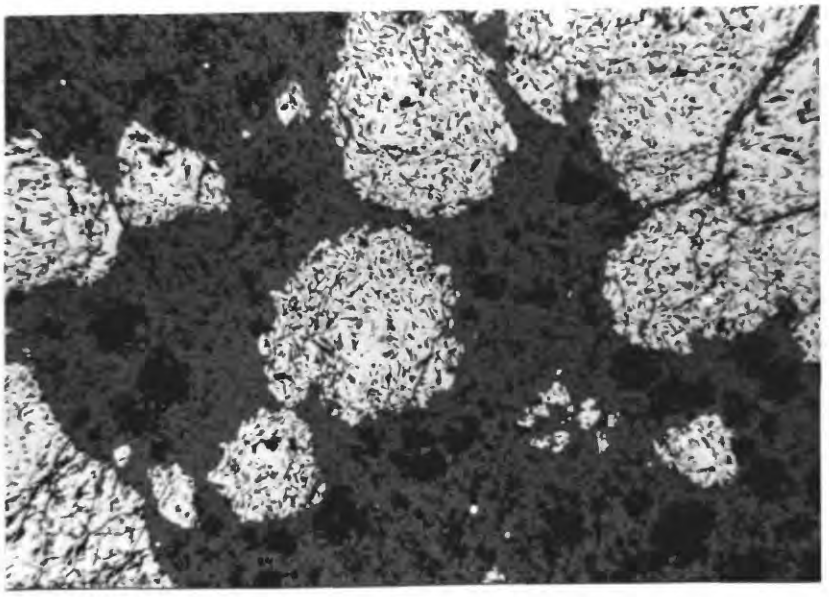

Figure 29

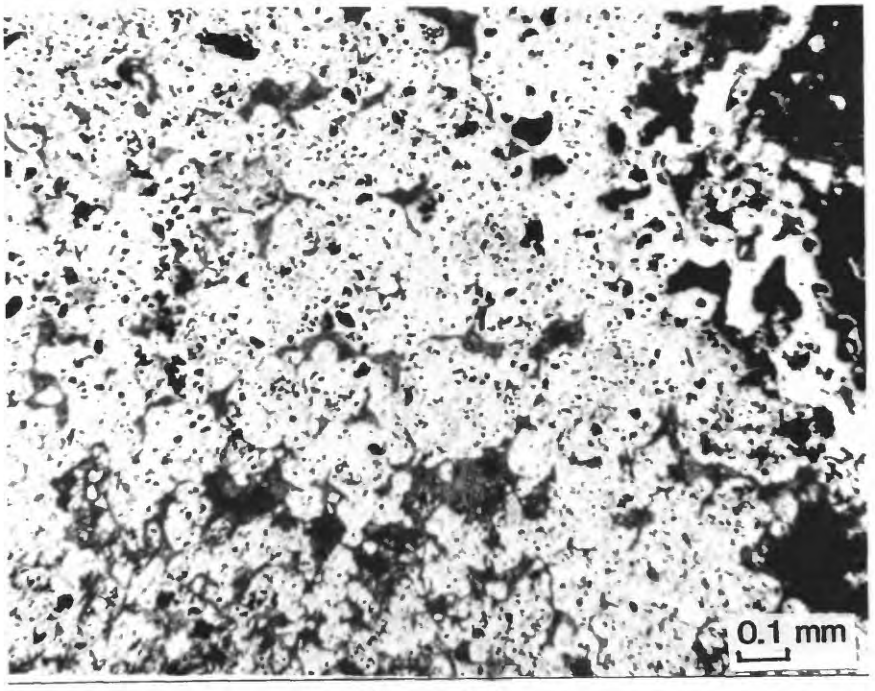

Figure 30

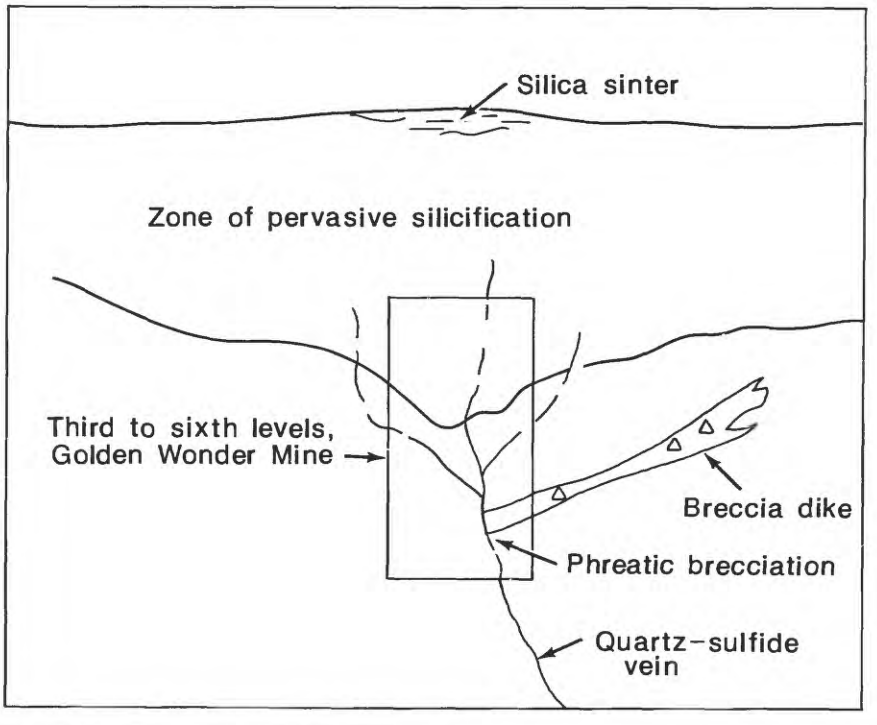

Figure 31

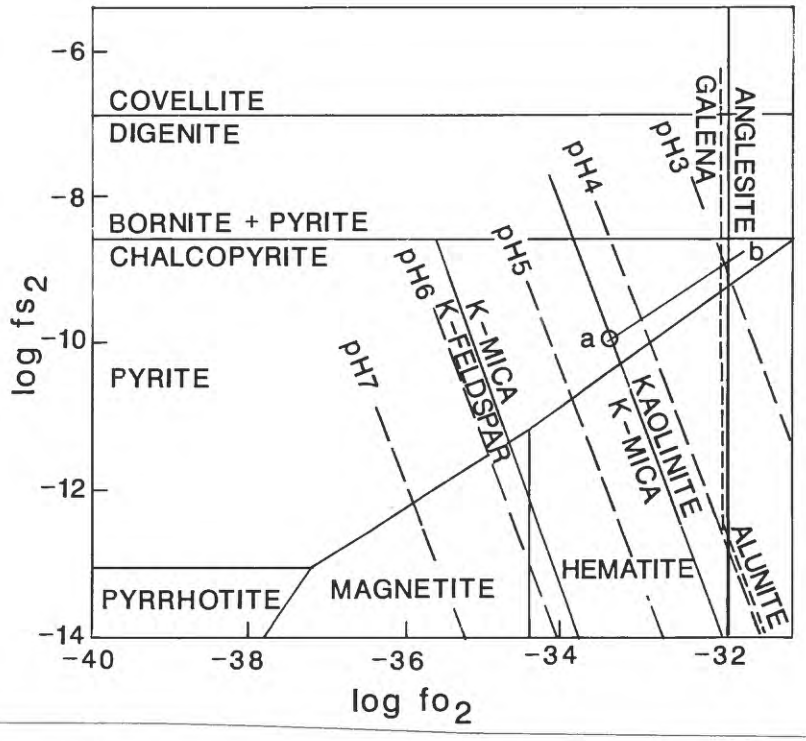

Figure 32

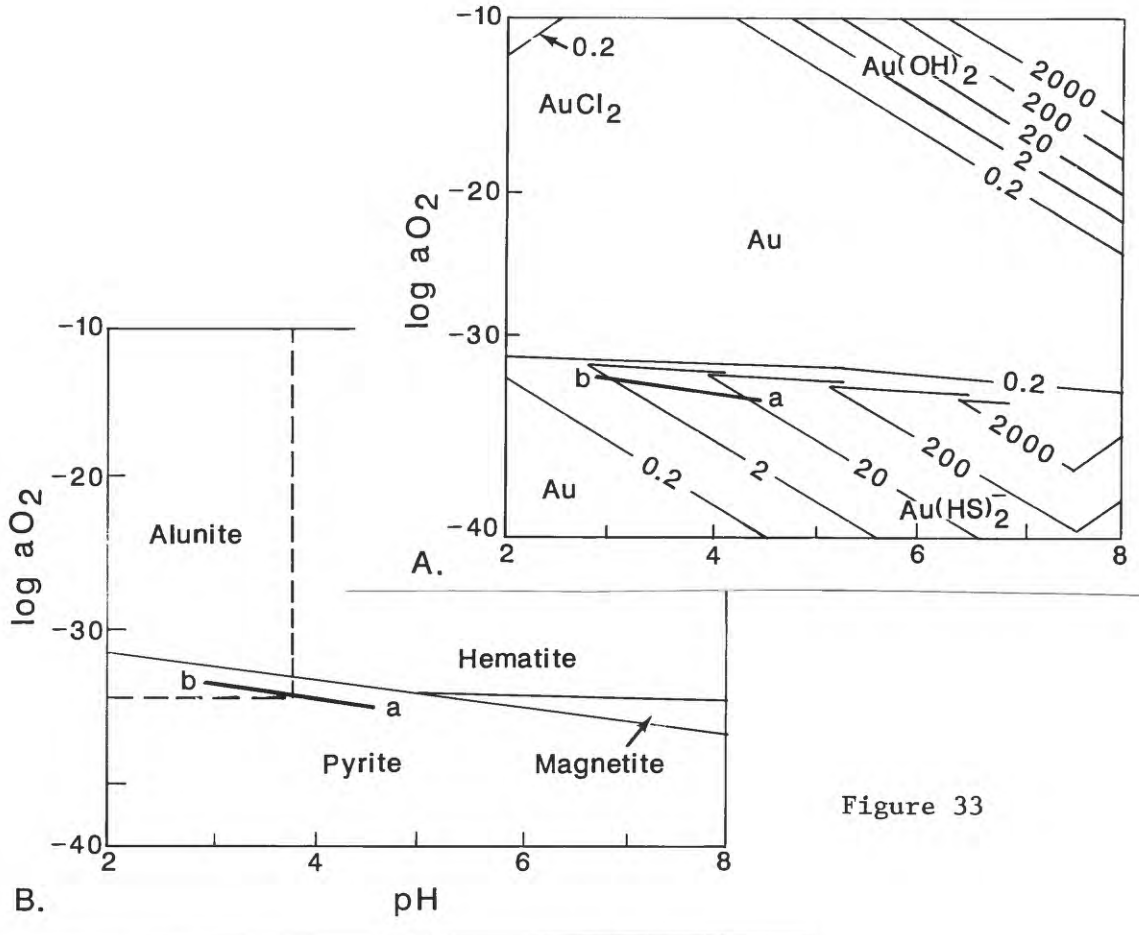

Figure 33

TABLE 1

MINERALOGY

MINERAL	FORMULA	MODE OF OCCURRENCE IN MINE										SLACK (1976)
		Possibly supergene	Epigenetic, in bedded alunite	Epigenetic, in quartzose sandstone	Clasts in quartzose sandstone	Crust on cavity wall, later filled with alunite	Crust on cavity wall, later filled with sandstone	Clasts in jasperoid-pyrite breccia	Quartz-pyrite-marcasite vein, sixth level	Breccia dikes, sixth and fourth levels	Wall rock alteration mineral	
hematite	Fe_2O_3	X										
tellurite	TeO_2	X										X(S)
melonite	$NiTe_2$		X									
sylvanite	$AuAgTe_4$		X									
tellurium	Te		X									
anglesite	$PbSO_4$	X	X			X						X(S)
wehrlite(?)	Bi_3Te_2		X									
tellurobismuthite	Bi_2Te_3		X									
anatase	TiO_2				X							
kaolinite	$Al_4(Si_4O_{10})(OH)_8$		X	X	X						X	X
monazite(?)	$(Ce,La,Y,Th)\ PO_4$				X							
alunite	$KAl_3(SO_4)_2(OH)_6$	X	X	X	X	X			X		X	
covellite	CuS	X	X	X		X	X					X(S)
petzite	Ag_3AuTe_2			X			X					X(?)
native gold	Au			X		X	X					X(S)
galena	PbS		X	X		X		X				X
luzonite	Cu_3As_S4		X			X						
"enargite"	Cu_SAsS_4			X			X					X
"tetrahedrite"	$(CuFe)_{12}Sb_4S_{13}$			X		X	X	X	X			X
sphalerite	ZnS		X	X		X		X	X	X		X
wurtzite	ZnS		X									
chalcopyrite	$CuFeS_2$		X	X		X	X			X		X
marcasite	FeS_2							X	X	X		X
pyrite	FeS_2		X	X	X			X	X	X		X
quartz	SiO_2				X				X	X	X	X
chert	SiO_2				X			X				X
sanidine	$KAlSi_3O_8$											
illite	$KAl_2(AlSi_3O_{10})(OH)_2$										X	
sericite	$KAl_2(AlSi_3O_{10})(OH)_2$										X	X
dickite	$Al_4Si_4O_{10}(OH)_8$										X	X
hinsdalite	$(PbSr)Al_3(PO_4)(SO_4)(OH)_6$	X										
cerussite	$PbCO_3$											X(S)
chalcocite	Cu_2S											X(S)
calaverite(?)	$AuTe_2$											X
krennerite	$AuTe_2$											X(?)
stibioluzonite	Cu_3SbS_4											X
arsenopyrite	FeAsS											X
bournonite	$PbCuSbS_3$											X
boulangerite	$Pb_5Sb_4S_{11}$											X
goldfieldite	$Cu_{12}Sb_4Te_3S_{16}$											X
calcite	$CaCO_3$											X

(S) = supergene

? = tentative identification